



Meteorological conditions and anomalies during the Intercontinental Chemical Transport Experiment–North America

Henry E. Fuelberg,¹ Michael J. Porter,¹ Christopher M. Kiley,¹ Jeremy J. Halland,¹ and Danielle Morse¹

Received 30 June 2006; revised 18 December 2006; accepted 17 January 2007; published 3 May 2007.

[1] Meteorological conditions are described during the Intercontinental Chemical Transport Experiment–North America (INTEX-NA) that was conducted over the United States during July and August 2004. Relatively zonal flow dominated the contiguous United States during the first 2 weeks of the mission, while a series of large amplitude troughs traversed the eastern half of the country during the final 4 weeks. These troughs were accompanied by cold fronts reaching the Gulf of Mexico, an uncommon occurrence during August. Frontal passages over the northeast were somewhat above average, but the short time interval between passages precluded the formation of stagnant high-pressure centers containing abundant pollution. Atmospheric chemistry during INTEX-NA was heavily influenced by record-breaking fires over Alaska and western Canada. Persistent high pressure over Alaska provided ideal conditions for the wildfires and for transporting their burning by-products southeastward toward the INTEX domain where they were sampled frequently by INTEX aircraft. Forward trajectories and satellite imagery showed that the plumes later were carried to parts of Europe, Africa, and even the Arctic. Deep convection and lightning were important factors during INTEX-NA. Cloud-to-ground (CG) lightning data show that horizontal patterns and numbers of lightning flashes during INTEX-NA are similar to those of 2003 and 2005. Statistics derived from 10 day backward trajectories indicate that the DC-8 often sampled lightning influenced air.

Citation: Fuelberg, H. E., M. J. Porter, C. M. Kiley, J. J. Halland, and D. Morse (2007), Meteorological conditions and anomalies during the Intercontinental Chemical Transport Experiment–North America, *J. Geophys. Res.*, *112*, D12S06, doi:10.1029/2006JD007734.

1. Introduction

[2] The Intercontinental Chemical Transport Experiment–North America (INTEX-NA) was conducted over the contiguous United States and adjacent areas during July and August 2004 [Singh *et al.*, 2006] as part of NASA's Global Tropospheric Experiment (GTE) [McNeal *et al.*, 1984]. INTEX-NA was a component of the International Consortium for Atmospheric Research on Transport and Transformation (ICARTT) whose goals were to execute a series of coordinated experiments to study the emissions of aerosols and ozone precursors, as well as their chemical transformations and removal during transport to and over the North Atlantic Ocean [Fehsenfeld *et al.*, 2006]. The specific goals of INTEX-NA were (1) to understand the transport and transformation of gases and aerosols on transcontinental and intercontinental scales and their impact on air quality and climate; (2) to quantify and characterize the inflow and outflow of pollution over North America;

and (3) to provide validation of ongoing satellite measurement programs such as Terra, Aura, and Envisat [Singh *et al.*, 2006].

[3] Meteorological conditions play an important role in determining the transport and distribution of many chemical species [e.g., Merrill *et al.*, 1997; Fuelberg *et al.*, 2003]. For example, atmospheric temperature and humidity affect chemical reaction rates and thereby influence the lifetimes of many species [e.g., Mauzerall *et al.*, 1998; Blake *et al.*, 2001; Martin *et al.*, 2002]. Precipitation can scavenge some species [e.g., Cohan *et al.*, 1999; O'Sullivan *et al.*, 1999], while lightning can create species such as nitrogen oxides [e.g., Lawrence *et al.*, 1994; Bond *et al.*, 2001]. Warm conveyor belts associated with middle latitude wave cyclones are an important mechanism for lifting polluted air to the middle and upper troposphere where they can be transported over long distances [e.g., Carlson, 1998; Wernli, 1997; Stohl, 2001; Cooper *et al.*, 2004; Eckhardt *et al.*, 2004; Kiley and Fuelberg, 2006]. Deep convection and smaller-scale turbulent mixing also transport surface-based species into the free troposphere [e.g., Maloney *et al.*, 2001].

[4] This paper describes the meteorological setting for INTEX-NA, including large-scale flow patterns, their depar-

¹Department of Meteorology, Florida State University, Tallahassee, Florida, USA.

tures from climatology, distributions of lightning, as well as several unusual aspects of the period, e.g., widespread wild fires over Alaska and Canada and summer cold fronts reaching the United States Gulf Coast. The overall goal is to assess the representativeness of INTEX-NA with respect to typical summertime conditions and thereby facilitate the interpretation of the INTEX chemical data.

2. Data and Methodologies

[5] INTEX-NA employed NASA's DC-8 flying laboratory to collect extensive in situ chemical and meteorological data. The eighteen science flights stretched from the eastern Pacific Ocean to the central Atlantic Ocean, and from southeastern Canada to the U.S. Gulf Coast [Singh *et al.*, 2006]. In addition, the Jet stream 31 (J31) aircraft flew over the Gulf of Maine with the goals of validating satellite retrievals of aerosol optical depth spectra and of water vapor columns, as well as measuring aerosol effects on radiative energy fluxes [Russell *et al.*, 2007]. Although this paper focuses on the INTEX flight domain, it also considers various upwind and downwind regions whose meteorology affected the INTEX domain.

[6] Means of meteorological quantities during the INTEX period as well as their departures from climatology were obtained from reanalysis data prepared by the National Centers for Environmental Prediction (NCEP) [Kalnay *et al.*, 1996] and available on the Web site of the NOAA-CIRES Climate Diagnostics Center (CDC) at URL <http://www.cdc.noaa.gov>. However, the data used to prepare our trajectories were from 0 hour analyses of the National Weather Service's Global Forecast System (GFS) which is a global spectral forecast model. The GFS data were available four times daily (0000, 0600, 1200, and 1800 UTC) with a T254 spherical harmonic triangular truncation, interpolated to a $1.0^\circ \times 1.0^\circ$ latitude-longitude horizontal grid. The vertical resolution includes 64 unequally spaced sigma levels. For a surface pressure of 1000 hPa, 15 levels of these levels are below 800 hPa to provide a good representation of low levels.

[7] Details about the current version of the GFS are available at <http://www.emc.ncep.noaa.gov/modelinfo/index.html>. Briefly stated, GFS represents the planetary boundary layer (PBL) using the first-order diffusion scheme of Troen and Mahrt [1986]. The PBL height is based on a bulk Richardson approach to iteratively estimate the height starting from the ground upward. Once the PBL height is determined, the profile of the coefficient of diffusivity is a cubic function of the height. A countergradient flux parameterization is based on fluxes at the surface and the convective velocity scale [Hong and Pan, 1996]. Shallow, nonprecipitating convection is parameterized as an extension of the vertical diffusion [Tiedtke, 1983]. The cloud base is determined from the lifting condensation level, and vertical diffusion is invoked between cloud top and bottom. GFS represents penetrative convection following Pan and Wu [1995] which is based on Arakawa and Schubert [1974] as simplified by Grell [1993] with a saturated downdraft. The temperature and moisture profiles are adjusted toward the equilibrium cloud function using the deduced mass flux. Only the deepest cloud is considered, not the spectrum of clouds. The cloud model incorporates a downdraft mecha-

nism as well as evaporation of precipitation; entrainment also is considered. Mass fluxes induced by the updraft and downdraft are allowed to transport momentum.

[8] Trajectories were calculated using a kinematic model, i.e., employing u , v , and w wind components from the GFS analyses. Additional details about our trajectory model are given in Fuelberg *et al.* [1996, 1999, 2000] and Martin *et al.* [2002]. Compared to earlier versions of the model, the current trajectories were not terminated if they intersected the lower boundary, but instead continued isobarically along the surface and possibly were lofted later by vertical motion, a procedure similar to Stohl *et al.* [1995]. Limitations of trajectories are described by Fuelberg *et al.* [2000], Maloney *et al.* [2001], Stohl [1998], and Stohl *et al.* [1995].

[9] Lightning data used in the study were available from the NASA Marshall Global Hydrology Resource Center and collected by the National Lightning Detection Network (NLDN) that is owned and operated by Vaisala Inc. Specifics about the network's operations and methodology are discussed by Cummins *et al.* [1998]. The network determines the location, time, and other characteristics of each cloud-to-ground (CG) flash. The detection efficiency and location accuracy of the NLDN have improved substantially since its inception in 1989. The latest system upgrade occurred during 2002. The network's current detection efficiency is 90–95%, and location is accurate to within 500 m over most of the country [Cummins *et al.*, 2006]. No corrections were applied to the data to compensate for variations in detection efficiency and location accuracy across the study area. This produces an underestimation of flash counts. Weak positive flashes (<15 kA) were deleted from the data set since they are thought to represent intracloud discharges. There currently is no way to detect total lightning (cloud-to-ground plus intracloud) over the total United States on a continuous basis.

3. Mission-Averaged Conditions

[10] Mission-averaged flow patterns describe the overall conditions that influenced transport during INTEX-NA. Figure 1 contains time-averaged data for the entire INTEX period (1 July to 15 August 2004). The sea level pressure analysis (Figure 1c) shows well developed subtropical anticyclones off the east and west coasts of the United States. With central pressures of ~ 1024 hPa, they are semipermanent features that exhibit little day-to-day fluctuations in strength or location. However, Figure 1f shows that the extension of the Bermuda High over the southeast United States is ~ 3 hPa weaker during INTEX than the long-term climatological average (1968–1996). Later sections will show that this characteristic of the Bermuda High had important implications for transport during INTEX. The Pacific anticyclone also is slightly weaker than normal. There are no quasi-permanent pressure centers over the landmass of North America during the composite INTEX period. Instead, the next section will show that there were numerous important transient systems that cancelled each other during the averaging procedure.

[11] The time averaged height analysis at 500 hPa ($\sim 18,000$ ft) (Figure 1b) contains the two subtropical anticyclones seen at the surface. In addition, a low-pressure trough is oriented along the eastern United States, and a

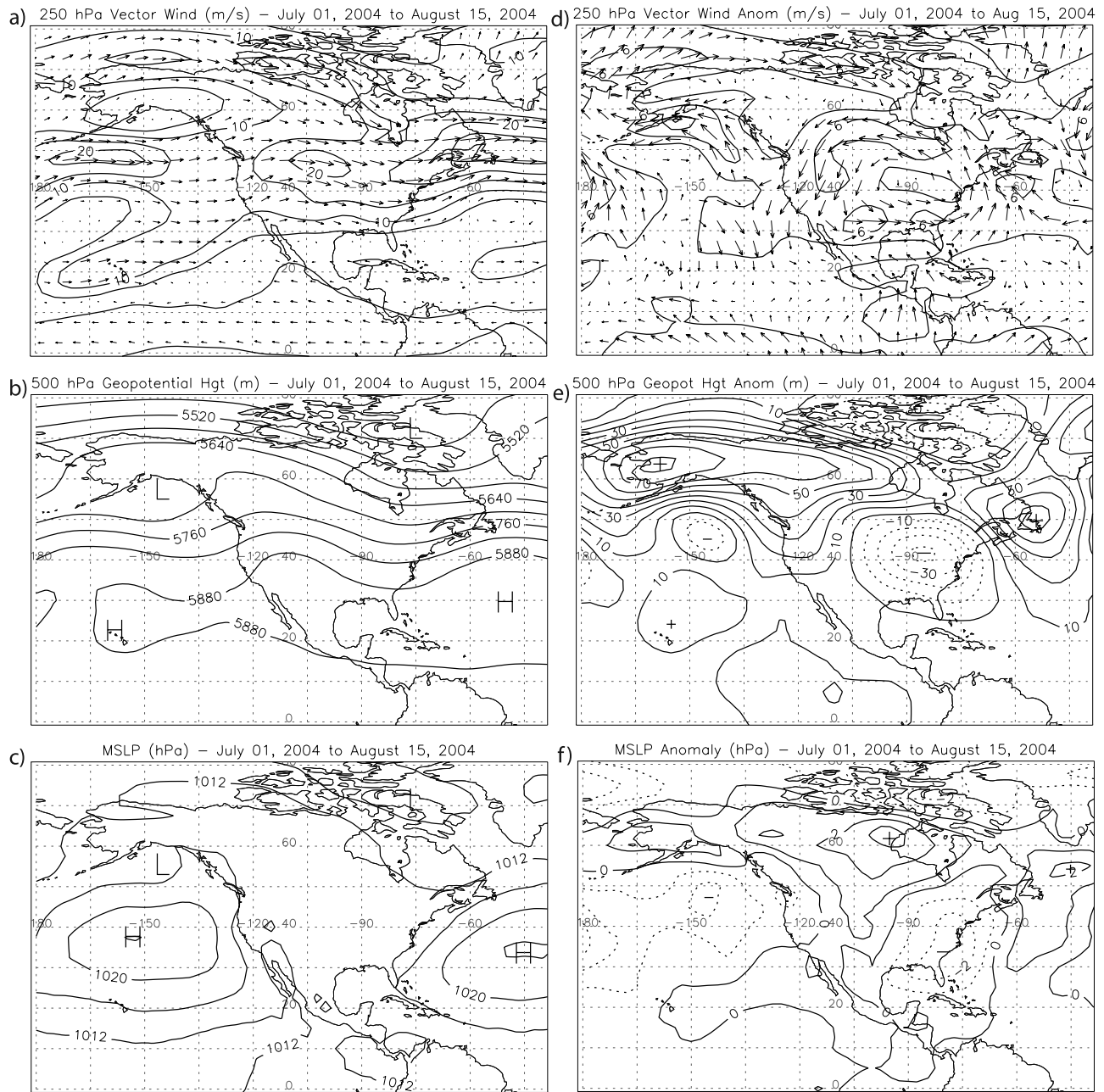


Figure 1. Mean conditions during the INTEX-NA period (1 July to 15 August 2004) and departures from the long-term climatology. (a) Mean vector winds and isotachs at 250 hPa ($\sim 34,000$ ft), (b) mean geopotential height pattern at 500 hPa ($\sim 18,000$ ft), and (c) mean sea level pressure (hPa). (d–f) Departures of the INTEX-NA period from the long-term climatology. The data were provided by the NOAA-CIRES Climate Diagnostics Center, Boulder, Colorado, from their Web site at <http://www.cdc.noaa.gov/>.

high-pressure ridge extends from the desert southwest into Alaska. The East Coast trough is ~ 40 m more intense than the climatological mean (Figure 1e), while the ridge over Alaska is ~ 70 m stronger than average. Finally, the closed low off the west coast of Canada is ~ 15 m more intense than typical. Since winds above the boundary layer blow approximately parallel to the height contours with higher heights to the right of the winds, Figure 1b reveals that the central United States on average experienced midtropo-

spheric flow from the northwest, thereby transporting air from Alaska and northwest Canada, while the eastern United States most often had flow from the southwest. Other implications of the height pattern are described in later sections.

[12] Figure 1a shows time averaged vector winds and isotachs at 250 hPa ($\sim 34,000$ ft). The mean position of the subtropical jet stream is from near Hawaii to the West Coast. Greatest mean speeds are ~ 10 m s $^{-1}$. The polar

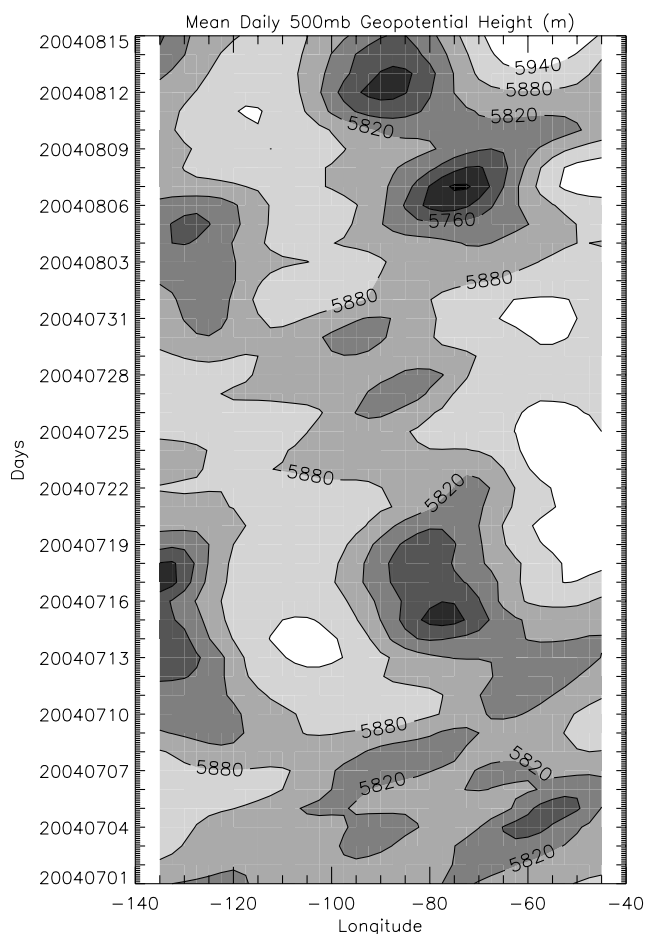


Figure 2. Time versus longitude (Hüvmüller) diagram of 500 hPa mean geopotential height at 40°N. The data were provided by the NOAA-CIRES Climate Diagnostics Center, Boulder, Colorado, from their Web site at <http://www.cdc.noaa.gov/>.

jet, located farther north, has two branches: one located just south of Alaska, with the second extending from extreme northern Alaska to Hudson Bay. These two branches merge near Maine and then stretch over the North Atlantic Ocean. Greatest mean wind speeds in both branches reach $\sim 15 \text{ m s}^{-1}$. As expected, wind directions at 250 hPa are similar to those below (Figure 1b). The anomaly analysis (Figure 1d) reveals that the subtropical jet stream and southern branch of the polar jet are near their climatological locations. However, the northern branch of the polar jet is somewhat stronger ($\sim 7 \text{ m s}^{-1}$) than normal.

4. Meteorological Peculiarities of the INTEX-NA Period

[13] The summer 2004 INTEX-NA period was unusual in several respects. Most of the contiguous United States was colder than normal; several cold fronts extended as far south as the Gulf Coast and central Florida; and Alaska was dominated by high pressure. The warm, dry conditions in the Alaskan high pressure favored a large number of thunderstorms and excessive lightning that ignited many wildfires whose influence was detected during many

INTEX flights. These meteorological aspects are described in the following sections.

4.1. Unusually Cool Summer Conditions in the Eastern United States

[14] The first 2 weeks of INTEX –NA (five science flights) are characterized by a series of shortwave troughs and ridges traveling from west to east across the contiguous United States. A time versus longitude plot of 500 hPa heights at 40°N (Figure 2) shows the progression of these waves across the region. This procession of troughs and ridges generally brought alternating periods of southwesterly and northwesterly middle tropospheric flow as they passed a location. The time averaged 500 hPa analysis during the initial 2 week period (Figure 3a) shows high pressure over the south, and nearly zonal flow over the remainder of the country. Height anomalies during the period (Figure 3c) generally are negative, but not excessively so (not more than -15 m). At the surface (not shown), the middle latitude systems were associated with cold fronts that carried polar air into the northern half of the United States.

[15] The remainder of the INTEX period (15 July to 15 August) exhibited considerably greater anomalies, both at the surface and aloft. Figure 4 shows 500 hPa height fields on three of the thirteen remaining DC-8 flight days (6 August, 20 July, and 25 July). An important feature is the large amplitudes of the low-pressure troughs over the eastern United States which extended as far south as the central Gulf of Mexico on several occasions (e.g., 6 August in Figure 4a). These high-amplitude troughs also are clearly depicted in the time-longitude plot (Figure 2). The 500 hPa time-averaged height pattern for this 4 week period (Figure 3b) shows the trough along the eastern United States and a ridge along the west coast, similar to that observed during the entire 6 week period (Figure 1b), thereby demonstrating the dominance of the final 4 weeks on the mission averaged flow. This series of large amplitude waves is unusual for summer. Height anomalies on individual days are as much as 200 m less than the norm (not shown), and as much as 60 m below normal for the monthlong period (Figure 3d). Typical summertime wave patterns exhibit smaller amplitudes that do not reach as far south. The high-pressure ridge along the west now is much stronger than during the first 2 weeks of INTEX. Later sections will show that this flow pattern was ideal for transporting smoke from wildfires in Alaska and northwestern Canada.

[16] Cold frontal passages over the East and Gulf Coasts were more frequent than normal during INTEX-NA. Table 1 gives the number of cold fronts that passed the northeast United States near Boston, as well as those passing the southeast near Atlanta, between 1 July and 15 August of years 2000–2005. Frontal locations were obtained from the National Weather Service’s archive of Daily Weather Maps http://docs.lib.noaa.gov/rescue/dwm/data_rescue_daily_weather_maps.html. Nine cold fronts passed the northeast during 1 July to 15 August 2004, with only 2005 exceeding this number. Conversely, only five fronts passed Boston during July 2000. Results for the southeast are even more impressive (Table 1), with more frontal passages (seven) than during any of the other years. The surface analysis for a representative strong frontal system over the southeast is

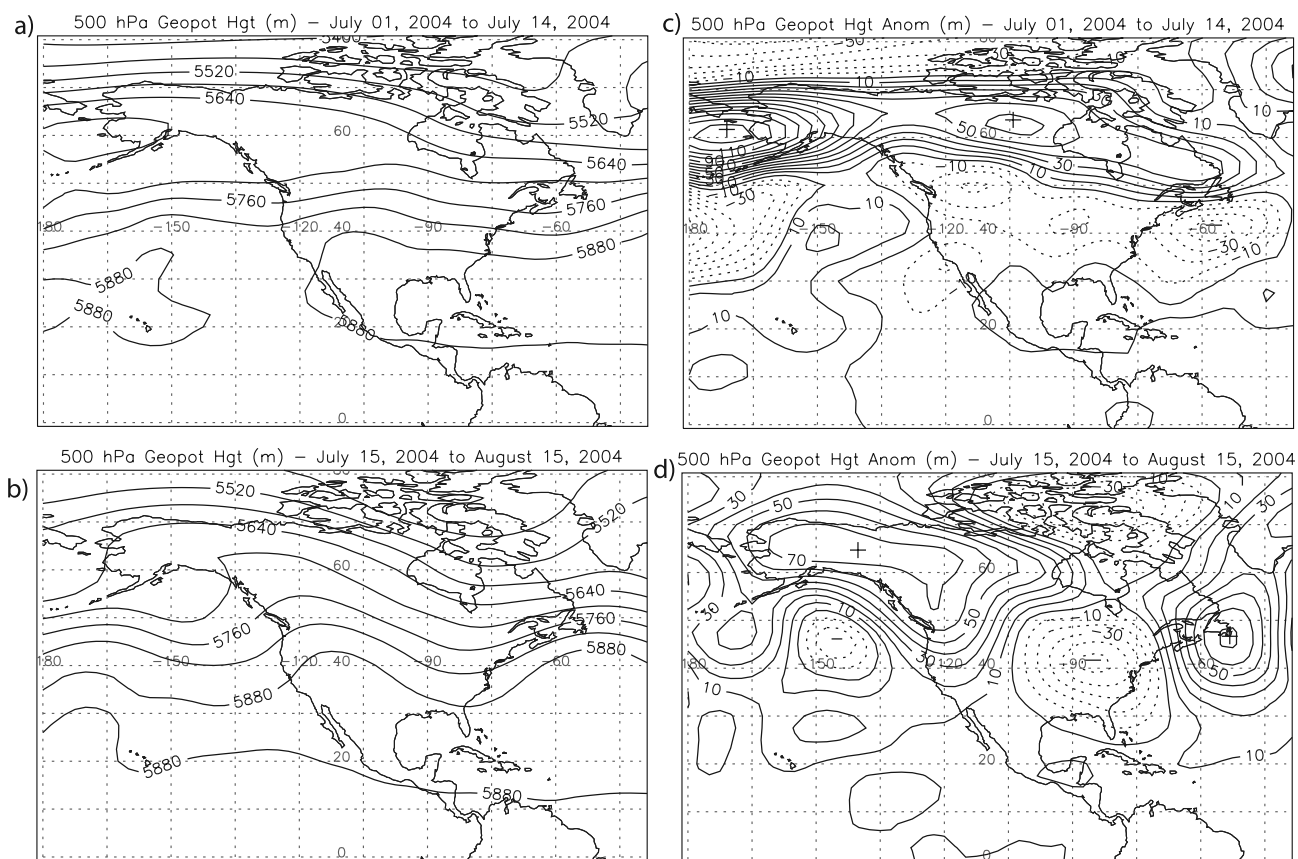


Figure 3. Mean geopotential heights at 500 hPa ($\sim 18,000$ ft) for the periods (a) 1–14 July 2004 and (b) 15 July to 15 August 2004. (c and d) Anomalies of these means from the long-term climatology. The data were provided by the NOAA-CIRES Climate Diagnostics Center, Boulder, Colorado, from their Web site at <http://www.cdc.noaa.gov/>.

shown in Figure 4d for 6 August. The cold front already has passed the northeast coast and now stretches from northern Florida, over the northern Gulf of Mexico, and into southern Texas. Well developed high pressure is located behind the front. These unusual cold fronts typically were preceded by widespread deep convection, and each brought somewhat cooler, drier air to the southeast, replacing the hot, humid conditions that are typical of summer. Each of the frontal cases was associated with a well developed trough aloft that provided the necessary upper level support for the surface fronts to extend so far south (e.g., Figure 4a).

[17] 20 July 2004 begins an interesting period when a strong summertime cold front and its associated upper level trough provided good sampling opportunities for the INTEX aircraft. The surface chart on 20 July (Figure 4e) shows the cold front extending off the East Coast and then southwest over northern Florida and just south of Louisiana. At 500 hPa (Figure 4b), the trough axis lies along the East Coast, producing southwesterly winds to its east. Strongest winds are located over the Canadian Maritimes (not shown). 20 July was the first in a sequence of 3 days when the DC-8 and NOAA WP-3D sampled air leaving the East Coast and crossing the Gulf of Maine toward the northeast.

[18] 25 July is the final example related to the numerous, strong frontal passages during INTEX. The surface analysis (Figure 4f) depicts the frontal system stretching along the

Atlantic Coast and southeastern United States, while the 500 hPa analysis (Figure 4c) shows a trough along the eastern United States. This case is interesting because of pollution transport across the Atlantic Ocean. The DC-8 sampled this air during its southern flight leg on 25 July, and again over Newfoundland on 28 July.

[19] The INTEX flight planning team had hoped to sample a stagnant high-pressure region over the northeast. Stagnant conditions would facilitate the buildup of pollution from the major urban areas which then would be swept northeastward by the next cold front where it could be further sampled by successive INTEX flights over the western Atlantic Ocean. Unfortunately, such stagnant conditions did not occur during the mission. Instead, the frequent cold frontal passages (Table 1) indicate an active summer period, with an average of only 4.6 days between successive cold frontal passages. Only the corresponding period of 2005 had a shorter span between fronts.

[20] Temperature, humidity, and precipitation play important roles in atmospheric chemistry. At the surface, the contiguous United States experienced its 16th coolest summer on record and seventh coolest August (NOAA, 2004, <http://www.noaanews.noaa.gov/stories2004/s2319.htm>). Minnesota had its coldest August on record, while six consecutive daily record minima were established at Meridian, Mississippi, and Mobile, Alabama. This was the

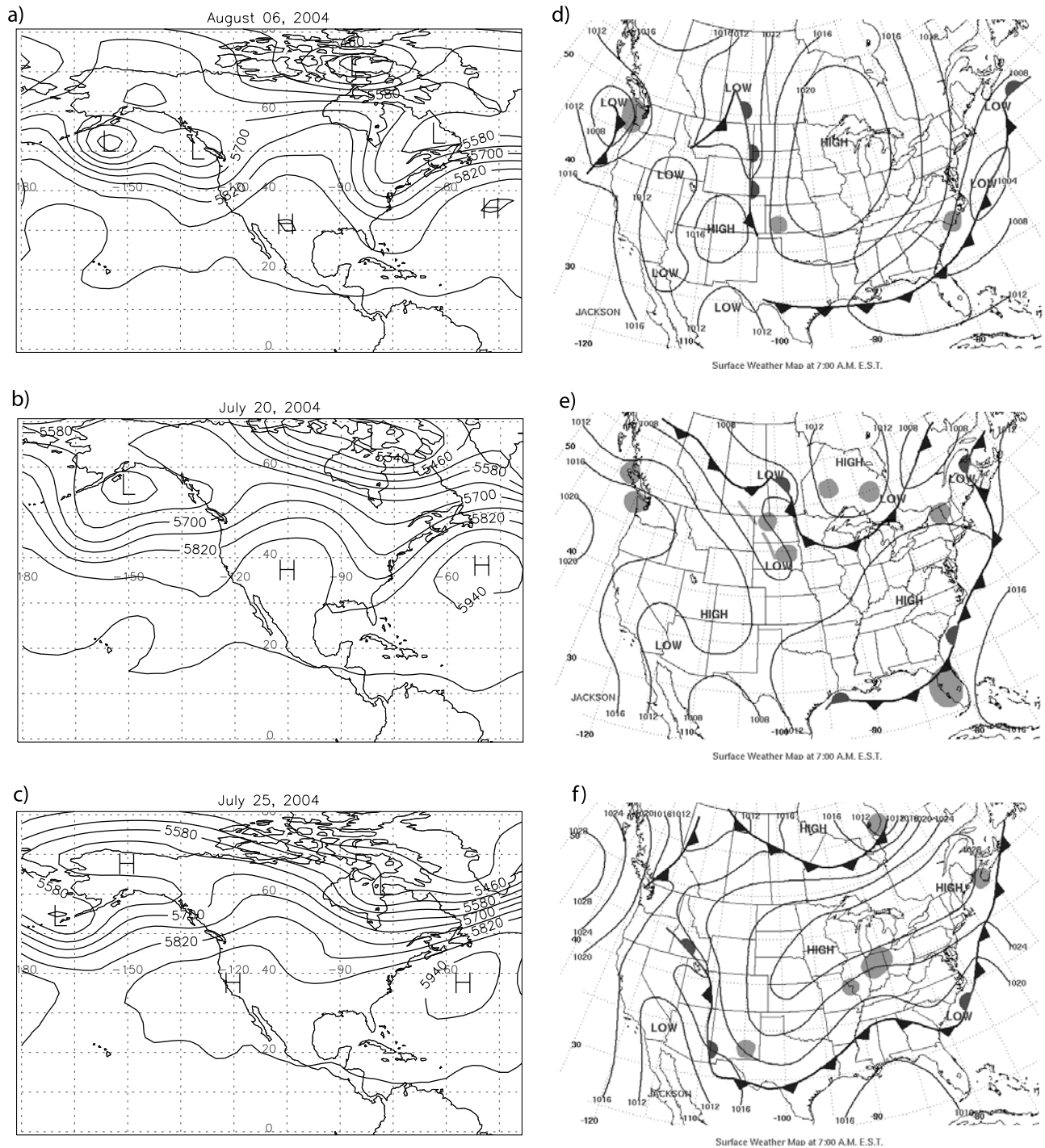


Figure 4. Geopotential height analyses at 500 hPa ($\sim 18,000$ ft) for (a) 6 August, (b) 20 July, and (c) 25 July. The data were provided by the NOAA-CIRES Climate Diagnostics Center, Boulder, Colorado, from their Web site at <http://www.cdc.noaa.gov/>. Surface analyses for (d) 6 August, (e) 20 July, and (f) 25 July prepared by the National Weather Service. Analyses are from the NOAA Central Library Data Imaging Project from their Web site at http://docs.lib.noaa.gov/rescue/dwm/data_rescue_daily_weather_maps.html.

longest summer cold spell in their observed weather histories dating back to the mid 1800s. Conversely, only three western states averaged much warmer than the long-term mean (years 1895–2003). The colder than normal conditions over most of

the country did not occur continuously, but mostly were due to several powerful cold outbreaks (Pennsylvania State University, 2004, http://pasc.met.psu.edu/PA_Climatologist/highlight/20041214/summer_2004.html).

Table 1. Number of Cold Fronts Passing Boston and Atlanta Between 1 July and 15 August in the Years 2000–2004^a

Year	Cold Fronts Passing Boston	Average Time Between Passages, days	Cold Fronts Passing Atlanta
2000	5	9.0	4
2001	7	6.6	5
2002	8	4.6	3
2003	7	5.8	5
2004	9	4.6	7
2005	12	4.0	3

^aThe average time (days) between frontal passages at Boston also is given. Frontal locations were obtained from the National Weather Service's archive of Daily Weather Maps http://docs.lib.noaa.gov/rescue/dwm/data_rescue_daily_weather_maps.html.

[21] Temperature anomalies aloft (Figure 5) show that much of the contiguous United States was colder than normal during the INTEX period, similar to that observed at the surface. At 850 hPa (Figure 5b), a large region east of the Continental Divide has below normal temperatures, with departures of $\sim 2.5^{\circ}\text{C}$ over Kansas and Illinois. Conversely, the West Coast is warmer than normal, with greatest departures over Washington. This general pattern continues in the middle troposphere (Figure 5a).

[22] Precipitation anomalies during the INTEX period are shown in Figure 6. Although the patterns are detailed because of the localized nature of summer precipitation, several general features are apparent. First, the West Coast is very dry during July, with much of California receiving less than 10% of normal precipitation. The northwest obtains rainfall during August, but the drought continues in California. Conversely, the northeast receives greater than average precipitation during both months, and this enhancement extends through the Carolinas and Florida during August because of the vigorous cold fronts that reach those areas. Finally, the Midwest tends to have above normal precipitation during July and August, although there are notable local exceptions. Detailed discussions of precipitation during both months can be found at <http://www.ncdc.noaa.gov/oa/climate/research/2004/jul/national.html#maps>.

[23] Anomalies of specific humidity in Figure 7 reveal departures during the INTEX period. At 850 hPa ($\sim 5,000$ ft, Figure 7b), the Mississippi River Valley is somewhat drier than normal, while the inverse is true for the Pacific Northwest. The southwest contains both drier and moister regions. Conditions at 500 hPa ($\sim 18,000$ ft, Figure 7a) are better defined, with most of the contiguous United States experiencing near or slightly above normal humidity. The large positive humidity anomalies along the East Coast (especially toward Florida) probably are a result of unusually strong advection from the Caribbean ahead of the cold fronts.

4.2. Unusually Warm, Dry Conditions in Alaska and Western Canada

[24] Excellent discussions of the 2004 Alaskan fire season and associated meteorological conditions are provided by *Richmond and Shy* [2005] and *Damoah et al.* [2005]. May 2004 was a wet period for most of Alaska, and few

fires occurred (not shown). Conditions then changed dramatically. The strong high-pressure ridge that developed over Alaska during the second half of June persisted several months (Figure 1). The mission averaged height anomaly at 500 hPa was ~ 70 m. Unlike typical summers, the persistent ridge prevented transient eastward moving low-pressure systems from entering the state. These systems would have brought cooler temperatures and widespread rainfall. Instead, a warm and often unstable air mass blanketed the area. Alaska during the second half of June was very warm and dry, with some areas breaking all time maximum temperatures (see <http://climate.gi.alaska.edu>) and recording only 25–50% of normal precipitation, the third driest summer on record [Rozell, 2004]. The fires that began during June grew explosively, fanned by surface winds of ~ 32 km h⁻¹ [Rozell, 2004]. The fires created dense smoke over nearby areas.

[25] Lower tropospheric temperatures during July were $\sim 3^{\circ}\text{C}$ above normal (Figure 5), and with the above normal humidity (Figure 7), many thunderstorms occurred. These thunderstorms produced widespread, often intense lightning on some days. For example, on 15 July, 9,022 cloud-to-ground flashes were detected over the state by the Alaskan lightning detection network. This was the greatest 24 hour total since the network became operational 25 years earlier.

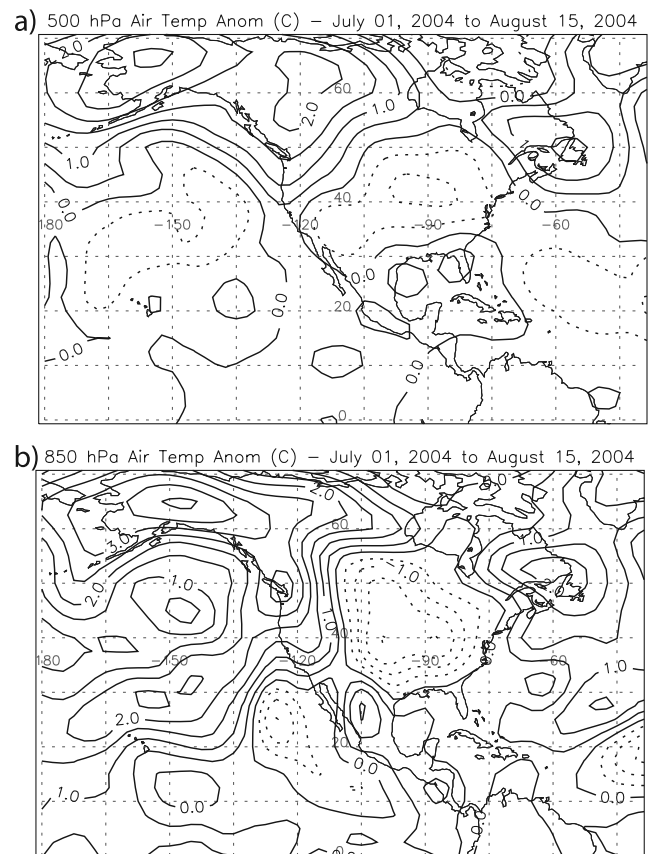


Figure 5. Departures of temperature ($^{\circ}\text{C}$) during the complete INTEX period from the long-term climatology at (a) 500 hPa and (b) 850 hPa. The data were provided by the NOAA-CIRES Climate Diagnostics Center, Boulder, Colorado, from their Web site at <http://www.cdc.noaa.gov/>.

Precipitation Percent of 1971-2000 Normal

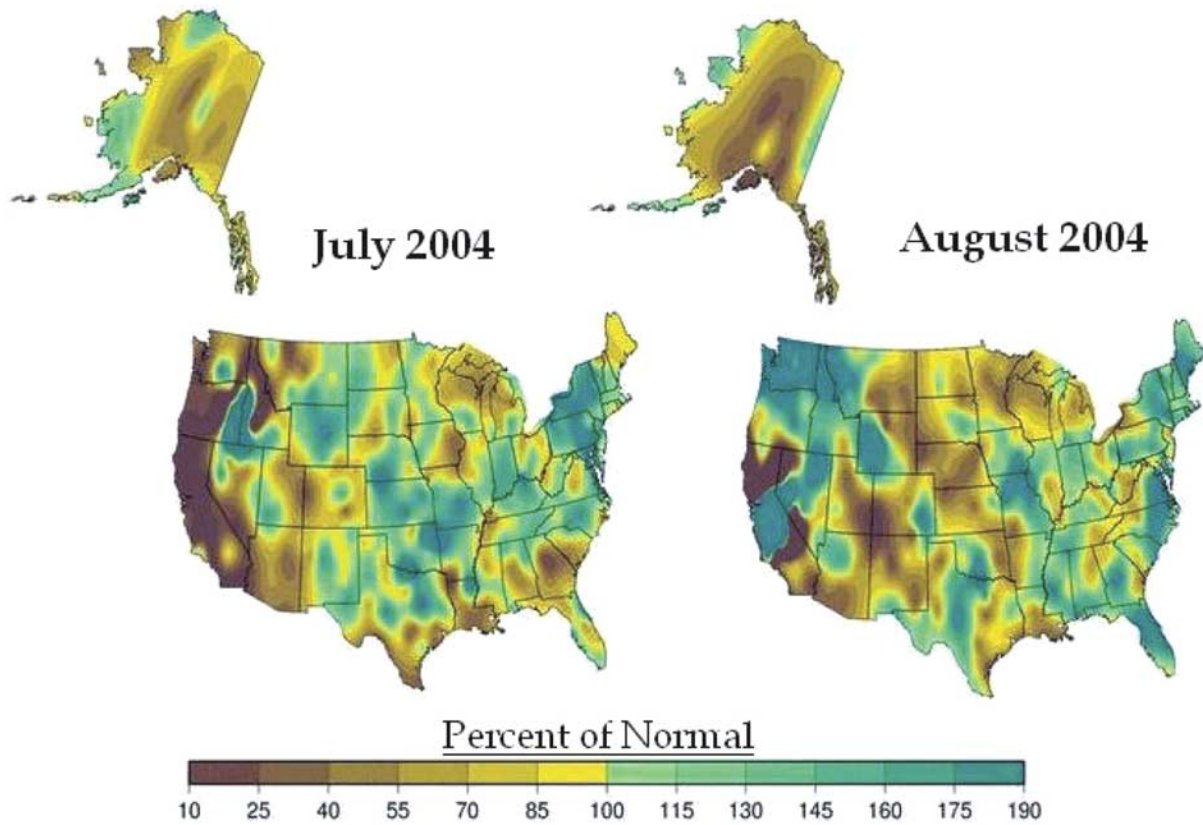


Figure 6. Percentage of normal precipitation during (left) July 2004 and (right) August 2004. Data are from the National Climatic Data Center at <http://www.ncdc.noaa.gov>.

Unfortunately, the storms did not produce sufficient rainfall to douse the existing fires, but instead their lightning started new fires. Rainfall amounts over much of Alaska were only 50–70% of normal (Figure 6). Fires in northwestern Canada began in mid July, i.e., later than those in Alaska. August also was a month of above normal temperatures and below normal precipitation (Figures 5 and 6), causing the fires to continue raging.

4.3. Record-Breaking Wildfires in Alaska and Western Canada

[26] Wildfires over portions of Alaska and western Canada are a common occurrence during the warm season. However, fire activity during the INTEX-NA 2004 period reached record-breaking proportions (Figure 8). Forest fire emissions not only affect the local surroundings, but also influence the atmosphere on regional scales [Tanimoto *et al.*, 2000; Kato *et al.*, 2002], continental scales [Wotawa and Trainer, 2000], and even hemispheric scales [Forster *et al.*, 2001; Wotawa *et al.*, 2001; Damoah *et al.*, 2004; Spichtinger *et al.*, 2004; Yurganov *et al.*, 2004; Novelli *et al.*, 2003]. Air quality in the United States is affected by wildfires in Canada [Wotawa and Trainer, 2000; McKeen *et al.*, 2002; DeBell *et al.*, 2004] and Siberia [Jaffe *et al.*, 2004]. The INTEX and ICARTT aircraft sampled the Alaskan and

Canadian plumes far downwind of their sources on numerous occasions.

[27] Figure 9a shows MODIS imagery of fire locations in Alaska on 1 July and (Figure 9b) near the border of Saskatchewan and Manitoba on 15 July. The widespread dense plumes of smoke are clearly visible. By the end of the year, the 707 fires in Alaska alone had burned 2.7×10^6 ha, which is 8 times the 10-year average (U.S. National Interagency Fire Center (<http://www.cidi.org/wildfire>)), surpassing the old record of 2×10^6 ha during 1957 [Damoah *et al.*, 2005]. In western Canada (Figure 9b), wildfires also were much greater than the 10-year average (Canadian Interagency Forest Fire Center). The total emission of CO due to fires in North America during 2004 has been estimated at 27 Tg [Turquety *et al.*, 2007] on the basis of burning inventory techniques. This total came from two major burning areas: Alaska-Yukon (21 Tg) and north-central Canada (6 Tg). Pfister *et al.* [2005] obtained the value 30 ± 5 Tg on the basis of inverse modeling of MOPITT CO observations. These record-breaking emissions represent a major perturbation to typical summertime conditions.

[28] The atmospheric flow patterns that created conditions conducive to the record-breaking fires also transported their burning by-products far downwind and into the

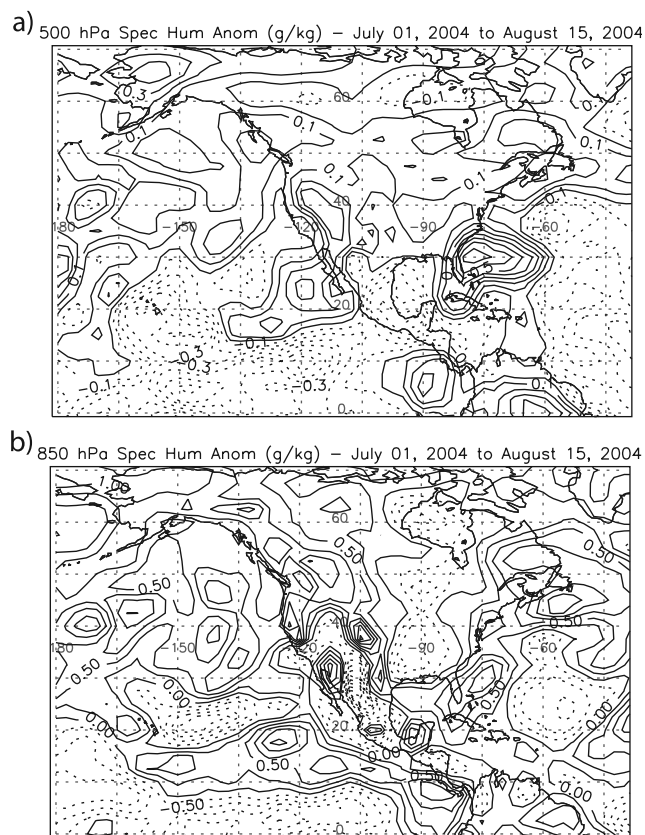


Figure 7. As in Figure 5 but for specific humidity (g kg^{-1}) at (a) 500 hPa and (b) 850 hPa.

INTEX and ICARTT domains. Specifically, persistent high-pressure ridging over Alaska and the West Coast, together with frequent troughs over the East Coast (Figures 1, 3, and 4), often carried the burning by-products eastward or southeastward. These plumes were sampled by the INTEX

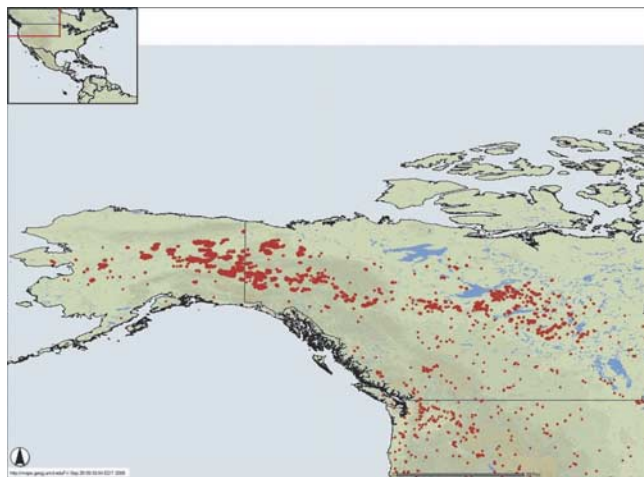


Figure 8. MODIS fire counts for the period 1 July to 15 August 2004. Data are from the MODIS Rapid Response System at the University of Maryland at <http://maps.geog.umd.edu/maps.asp>.

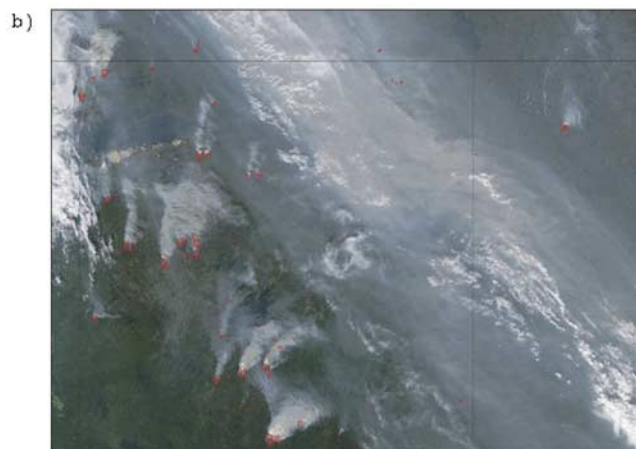
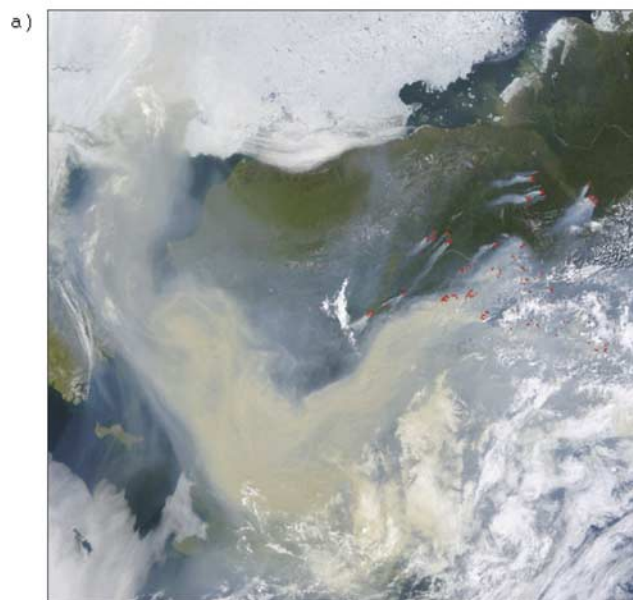


Figure 9. (a) MODIS images showing wildfire locations and smoke plumes over (a) Alaska and northwestern Canada on 1 July 2004 and (b) northwest Canada on 25 July 2004. Images were provided by NASA at <http://earthobservatory.nasa.gov/NaturalHazards>.

DC-8 on numerous flights. The plumes reached southern Texas and Louisiana on some days (not shown), while Figure 10 shows the smoke plume over the Labrador Sea off the coast of Newfoundland on 19 July. Figure 11 shows backward trajectories along three segments of flight 9 in this area on 18 July, 1 day earlier than the image, but still containing the major smoke plume. These trajectories, arriving at the DC-8 at altitudes ranging from 500 to 300 hPa, clearly show long-range transport from the fire regions in Figure 8. In this example the DC-8 sampled air that had originated over the burning areas 4 to 10 days earlier, depending on aircraft altitude and meteorological conditions. The burning by-products also traversed several different routes, reaching the Gulf of Mexico Coast during mid-July. Backward trajectories (not shown) reveal that the



Figure 10. MODIS image showing a smoke plume over the Labrador Sea off the coast of Newfoundland on 19 July 2004. The image was provided by NASA at <http://earthobservatory.nasa.gov/NaturalHazards>.

smoke over Arkansas, Louisiana, southeastern Texas, and coastal Mississippi had traveled eastward over Canada and then southward along the Mississippi River, a distance of several thousand kilometers. This type of southward extension was sampled by the DC-8 during several INTEX flights (not shown). For example, *Morris et al.* [2006] showed that Alaskan and Canadian forest fires exacerbated ozone pollution over Houston, Texas, on 19–20 July 2004.

[29] The smoke plumes from Alaska and western Canada were clearly visible to those onboard the DC-8. For example, Figure 12 is a photograph taken from the cockpit of the DC-8 as it approached Portsmouth, New Hampshire, on 20 July (flight 10). The aircraft's altitude at the time was approximately 600 hPa ($\sim 14,000$ ft). The plume is highlighted against cumulus clouds in the background, and careful inspection reveals one thick, dense pollution layer, as well as several thinner, weaker layers. Backward trajectories from the area of the smoke plume in Figure 12 are shown in Figure 13. The polluted air observed and sampled by the DC-8 originated over regions of fire activity in Alaska 6–7 days earlier (Figure 8).

[30] The long-range transport of smoke observed during INTEX-NA is consistent with recent studies showing that although burning by-products are emitted in the boundary layer, the intense convection over fires can transport the by-products rapidly to much higher altitudes where horizontal winds are stronger [*Fromm et al.*, 2000, 2005; *Fromm and Servranckx*, 2003]. Using a chemical transport model, *Colarco et al.* [2004] showed that an injection height of 2–6 km produced the best agreements with observed conditions for Canadian wildfires during July 2002. *Pfister et al.* [2005] distributed the 2004 emissions uniformly up to height of 400 mbar to achieve best agreement with a chemical transport model.

[31] Deep convection that is triggered or enhanced by forest fires (pyroconvection) can even deposit burning by-products in the upper troposphere and lower stratosphere [*Fromm and Servranckx*, 2003, 2005; *Livesey et al.*, 2004;

Immler et al., 2005; *Jost et al.*, 2004]. *Andreae et al.* [2004] proposed that burning-derived aerosols can affect cloud microphysics such that latent heating at high altitudes is enhanced, thereby increasing the height of a storm.

[32] *Damoah et al.* [2006] showed that strong pyroconvective events occurred during the Alaskan and Canadian wildfires of 2004. In some cases, convective cloud tops as cold as -60°C were almost coincident with major fire regions. That convection penetrated the lower stratosphere, reaching 3 km above the tropopause. The downstream INTEX and ICARTT data show evidence of these byproducts as high as 10 km [*de Gouw et al.*, 2006]. As a result of the high-altitude CO observations, *Turquety et al.*'s [2007] chemical transport modeling of 2004 Alaskan wildfires distributed emissions as 40% in the boundary layer, 30% in the middle troposphere, and 30% in the upper troposphere. This distribution provided the best agreement with CO measurements from the MOPITT spaceborne instrument [*Deeter et al.*, 2003].

[33] Papers in this special INTEX section that investigate wildfire emissions include A. D. Clarke et al. (Aerosol from biomass burning and regional pollution over North America during INTEX-NA: Humidity response and the wavelength dependence of scattering and absorption, submitted to *Journal of Geophysical Research*, 2006), and *Pfister et al.* [2006].

[34] One of the goals of ICARTT was for the European aircraft to sample air over the eastern Atlantic Ocean that had been sampled previously by the INTEX DC-8 over the United States or the western Atlantic Ocean. This multiple sampling would permit the evolution of plume chemistry to be studied. Since it was unlikely that the European aircraft would sample the identical parcels sampled earlier, this approach was denoted “quasi”-Lagrangian, instead of truly Lagrangian. The INTEX and ICARTT aircraft conducted several “wing tip to wing tip” intercomparison flights to insure that the data from each aircraft could be used in the quasi-Lagrangian experiments. The pilots went to great lengths to provide minimal aircraft separation during the intercomparisons (Figure 14).

[35] Results indicate that the quasi-Lagrangian objective was met to varying degrees during a number of flights. Specifically, air sampled by the DC-8 on 6, 8, 10, 12, 15, 18, 25, and 28 July and 14 August appeared to be transported to Europe and beyond. For example, Figure 15 shows 10 day forward trajectories from the three flight segments shown earlier in Figure 11. Depending on the synoptic situation, the burning plumes crossed the Atlantic Ocean in as little as 3 days, reaching England, the Mediterranean Sea, and Asia. Many of the parcels remained at approximately the same altitude at which they were sampled by the DC-8; however, some experienced considerable subsidence, especially those in Figure 15c) as they passed east of a high-pressure region. One also should note that some trajectories extend into the Arctic regions, contributing to Arctic haze [*Stohl*, 2006]. It is clear that major pollution from any location on the Earth truly is transported on a hemispheric scale.

4.4. Lightning During INTEX-NA

[36] Lightning generally is confined to deep convective clouds that contain strong updrafts and have ice in their

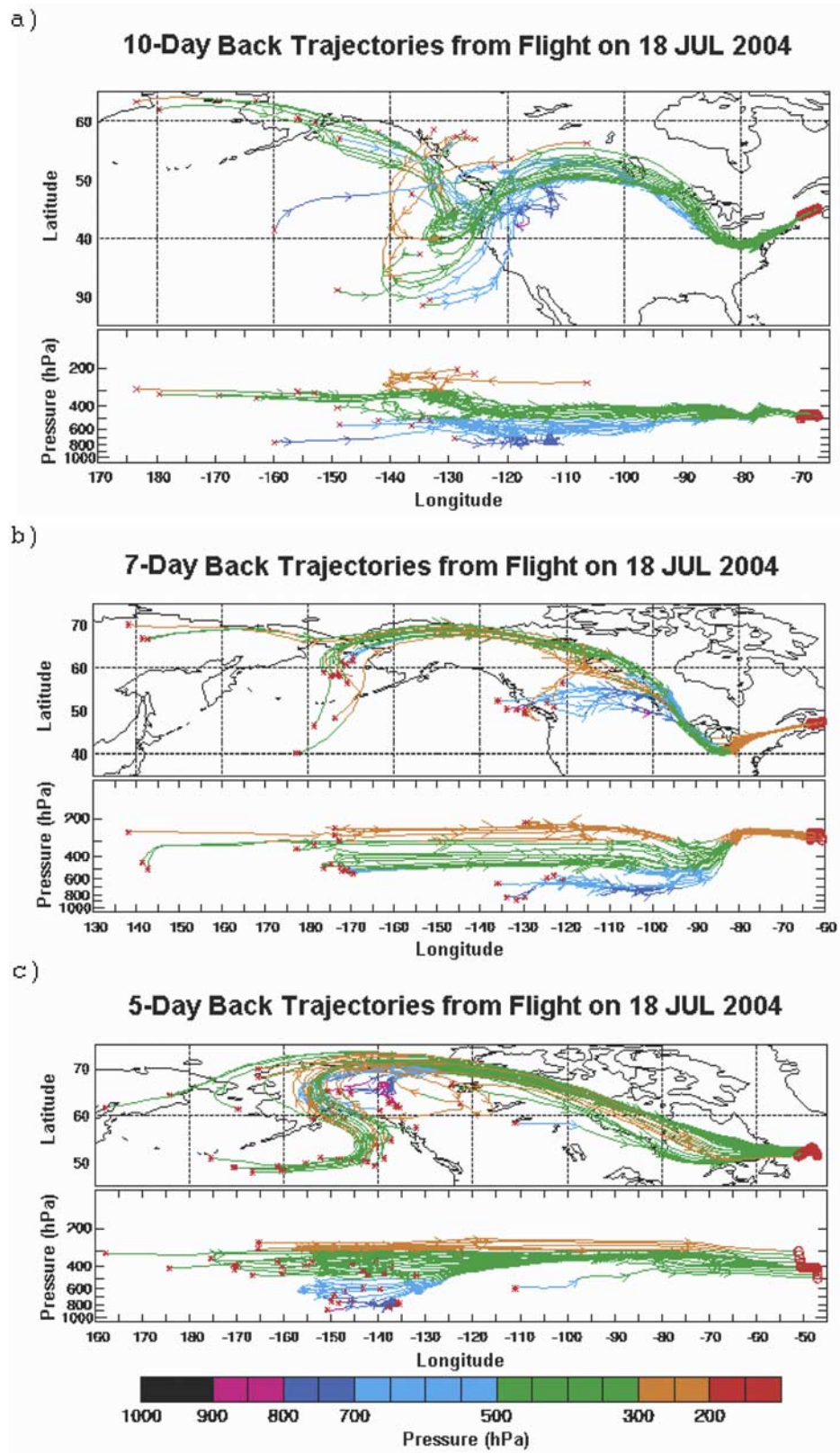


Figure 11. Horizontal and vertical plots of backward trajectories from three legs of the DC-8 flight on 18 July 2004 when a biomass burning plume was encountered over the Labrador Sea, (a) 10 days back arriving at the DC-8 near 500 hPa, (b) 7 days back arriving at the DC-8 near 300 hPa, and (c) 5 days back arriving at the DC-8 between 500 and 300 hPa (~18,000–30,000 ft). The Florida State University archive of INTEX-NA trajectory plots is available on the Web at <http://fuelberg.met.fsu.edu/research/intexa>.



Figure 12. Photo taken from the cockpit of the DC-8 by the lead author during the flight on 20 July 2004 as the aircraft was approaching Portsmouth, New Hampshire. The plume is located ahead of a developing cumulus cloud. Note the thick and several thin layers of pollution.

upper reaches. Figure 16 shows the horizontal distribution of cloud-to-ground lightning over the contiguous United States during the composite 6 week INTEX period, where the flashes have been counted over boxes that are 0.1° latitude (11 km) on each side. Florida and the eastern Gulf Coast experience the greatest lightning over the contiguous states during INTEX, with large areas exceeding 500 flashes per 11 km square box. This lightning is due to cold fronts that

atypically reached this far south (section 4.1) and due to sea breeze circulations [e.g., *Lericos et al.*, 2002; *Smith et al.*, 2005], afternoon heating, and other small-scale forcing mechanisms. The Great Plains and Mississippi and Ohio River Valleys also experience abundant CG lightning that often was due to passing transient synoptic systems. Conversely, there is much less lightning over the West Coast, Pacific Northwest, and New England. The INTEX-NA lightning pattern has many similarities to the mean annual flash densities calculated by *Orville and Huffines* [2001] during the 1989–1998 period. Thus INTEX lightning distributions appear representative of climatology.

[37] Historical CG lightning counts are presented in Table 2 for a rectangle enclosing the contiguous United States and the area just north of the Great Lakes ($66\text{--}126^\circ\text{W}$, $25\text{--}50^\circ\text{N}$). The NLDN underwent a major upgrade during 2002, yielding an improved detection efficiency and location accuracy [*Cummins et al.*, 2006]. These earlier data are not considered here since the resulting flash counts would be inconsistent with the more recent results. July 2004, with 7,691,566 flashes, had the greatest number of the three year period. Conversely, 1–15 August 2004 had the smallest total of the three years. Although the overall INTEX period, with 10,692,608 CG flashes, had the smallest flash count of the most recent 3 years, the difference is not great. Thus 2004 appears typical of at least the most recent years.

[38] It is important to note that on an annual basis there are 2.64 to 2.94 cloud discharges for every cloud to ground flash over the continental United States [*Boccippio et al.*, 2001; *Bond et al.*, 2001]. However, more recent data suggest that this number is even greater during the summer, approximately 4.2 (D. Boccippio, personal communication,

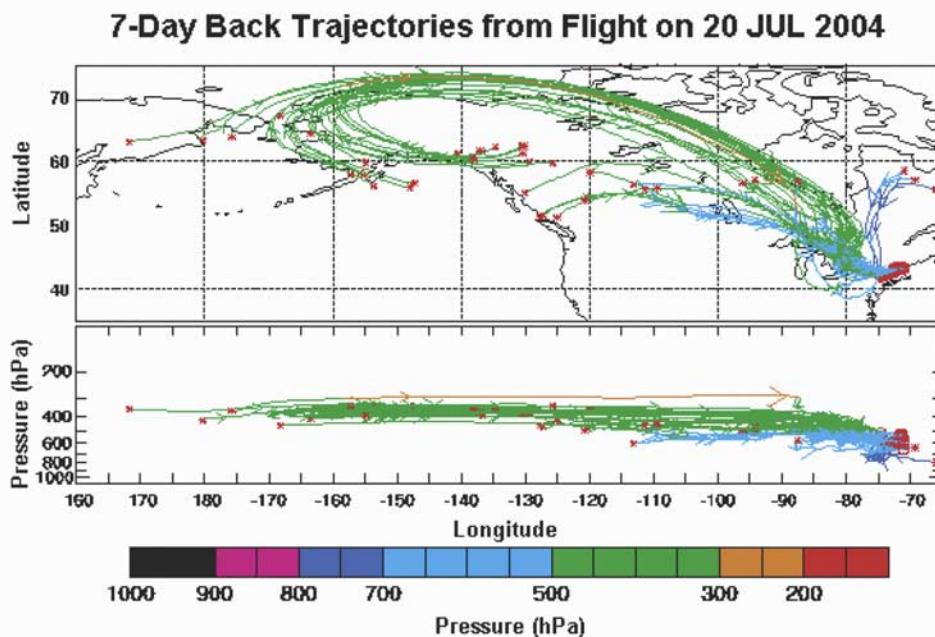


Figure 13. Horizontal and vertical plots of 7 day backward trajectories arriving at the DC-8 at the location of the observed plume in Figure 12. The trajectories arrive at the height of the aircraft (~ 600 hPa, $\sim 14,000$ ft). Note the trajectory origins over the wildfire regions of Alaska.



Figure 14. Photo taken from the cockpit of the DC-8 by the lead author showing the intercomparison flight with the NOAA P-3B aircraft on 7 August 2004.

December 2005). Thus the total number of CG, intercloud, and intracloud flashes likely is approximately 57 million during INTEX-NA. Although some satellite sensors detect total lightning, they are in polar orbits, crossing a given location only twice daily. Furthermore, the northern extents of their orbits do not cover the entire INTEX area. Thus satellite-derived satellite data cannot be used to provide a better estimate of total lightning during INTEX.

[39] *Bond et al.* [2001] assumed an NO production rate of 6.7×10^{26} molecules for each CG flash and 6.7×10^{25} molecules for each cloud flash based on *Price et al.* [1997]. *Bond et al.* [2001] concluded that regional emissions of NO_x by lightning can be significant during the summertime and may play a major role in ozone formation in the free troposphere. However, recent research by *DeCaria et al.* [2000, 2005], *Fehr et al.* [2004], and *DeCaria et al.* [2005], indicates that cloud flashes on average are nearly as productive as CG flashes in producing NO. In any event, the current data certainly suggest that lightning was a major producer of NO_x during INTEX-NA [*Cooper et al.*, 2006].

[40] Figure 17a contains CG flash counts over the contiguous United States for each INTEX day in the area described above. The first half of July was the most lightning prolific period, with much of the lightning occurring east of the Mississippi River (not shown). This major lightning activity occurred during a period of relatively zonal flow (Figure 3). The second half of July and first half of August contained less lightning, although there were several periods of intense activity that corresponded to the southward extending cold fronts and major sea breeze activity. As noted earlier, record-breaking lightning counts also occurred over Alaska and western Canada during INTEX; however, those data are not shown in Figure 17.

[41] The diurnal distribution of CG lightning over the INTEX area is shown in Figure 17b. Maximum activity occurs between 2200 and 2300 UTC (late afternoon), corresponding to the period of greatest low-level hydrostatic

instability. Conversely, the minimum is near 1500 UTC (early morning) when stable conditions or even temperature inversions usually are present. The INTEX diurnal lightning distribution is similar to that of climatology [*Orville and Huffines*, 2001].

[42] The DC-8 flew near active deep convection on several missions and detected convective chemical signatures on many other flights. DC-8 flights 7 and 12 on 12 and 25 July, respectively, are good examples of when intense convection was sampled both during and prior to the flight. 12 July was the third most active lightning day during INTEX-NA (Figure 17a), occurring during the general period of greatest flash activity. The DC-8's track over the southeast and Midwest is superimposed on a color coded hourly lightning distribution in Figure 18a. The similarity of colors between the flight track and the lightning over the southern Appalachians indicates that the DC-8 was flying near the time of lightning occurrence. Flight 12 (Figure 18b) also sampled recent lightning over the Appalachians. This flight occurred during a secondary peak in flash counts (Figure 17a).

5. Quantifying the DC-8's Sampling of Convection and Lightning

[43] It is informative to quantify the variety of parcel histories sampled by the DC-8 during the eighteen science flights of INTEX-NA. E. V. Browell et al. (personal communication, 2005) used data from the Differential Absorption Lidar (DIAL) instrument to perform large-scale air mass characterizations during INTEX. We have used a different approach, utilizing backward trajectories at 1 min intervals along each DC-8 flight leg. Our trajectory methodology was described in section 2, and the complete trajectory data set is available at <http://www-air.larc.nasa.gov/cgi-bin/arcstat>, with images available at <http://fuelberg.met.fsu.edu/research/intexa>. Hourly back positions of all 9,409 DC-8 trajectories were compared with fields from the GFS model (described in section 2), NLDN lightning data, and MODIS fire count data. The first encounter with several types of environments was recorded (Table 3). Encounters were considered within the area 25–50°N and 66–126°W. This procedure does not quantify parcels that were affected by multiple processes such as biomass or urban plumes later impacted by convection and/or lightning or mixing with stratospheric air. However, discussions during the flights indicated that these multiple influence likely were a common occurrence.

[44] To determine boundary layer encounters, each trajectory's pressure was compared to the closest model-derived PBL height. A residual layer encounter was reported if the trajectory passed above the PBL, but below the level of the previous day's boundary layer. Stratospheric encounters were located by comparing the trajectory's pressure with the model reported tropopause height. Convective influence was assumed if the GFS grid point nearest the trajectory had convective precipitation during the previous hour and the trajectory passed below the level of the highest cloud tops. If no high clouds were reported, convective influence was assumed if the trajectory encountered convective precipitation and was below 500 hPa.

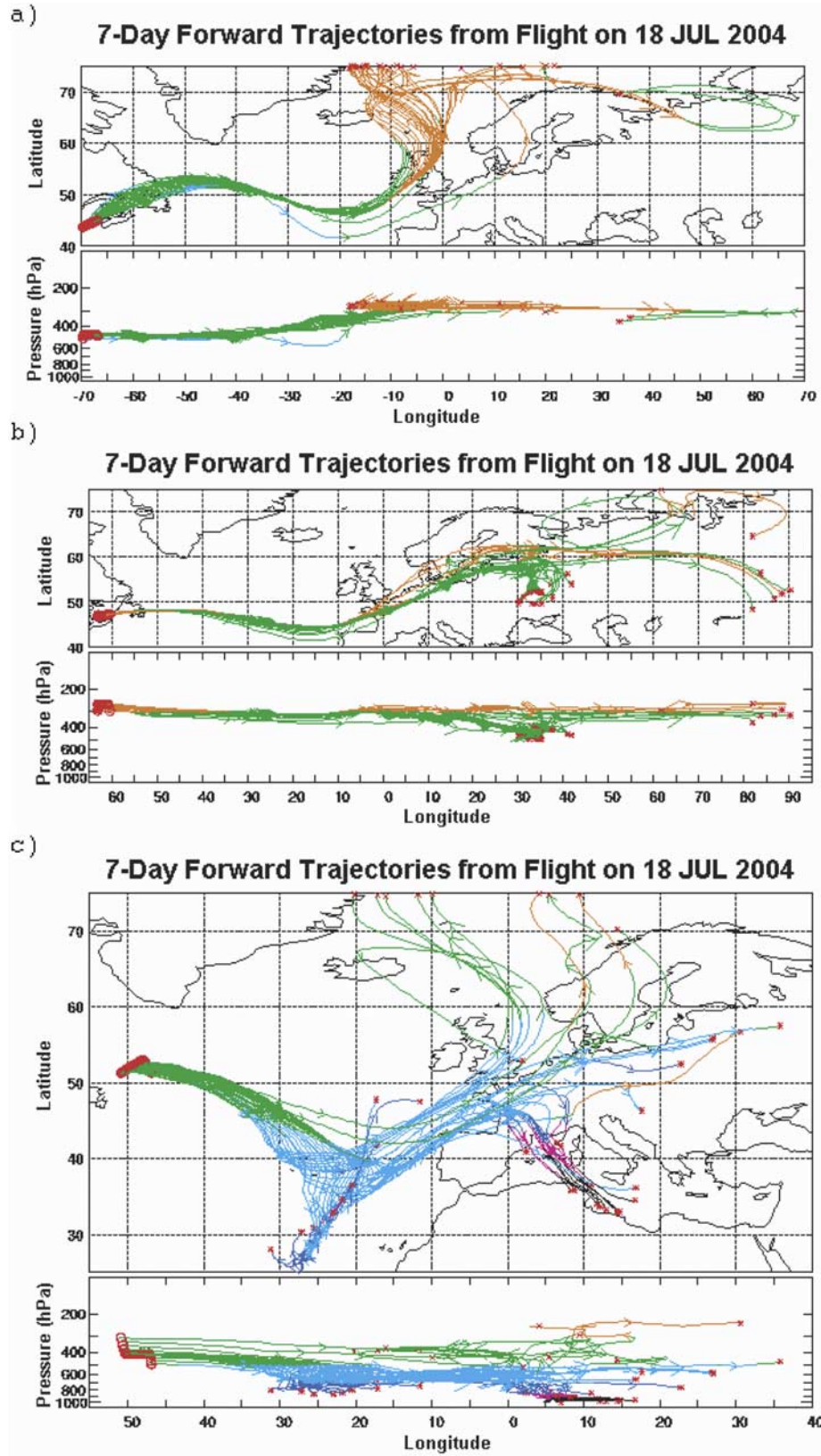


Figure 15. Horizontal and vertical of plots of 7 day forward trajectories beginning on 18 July 2004 from flight legs shown in Figure 11.

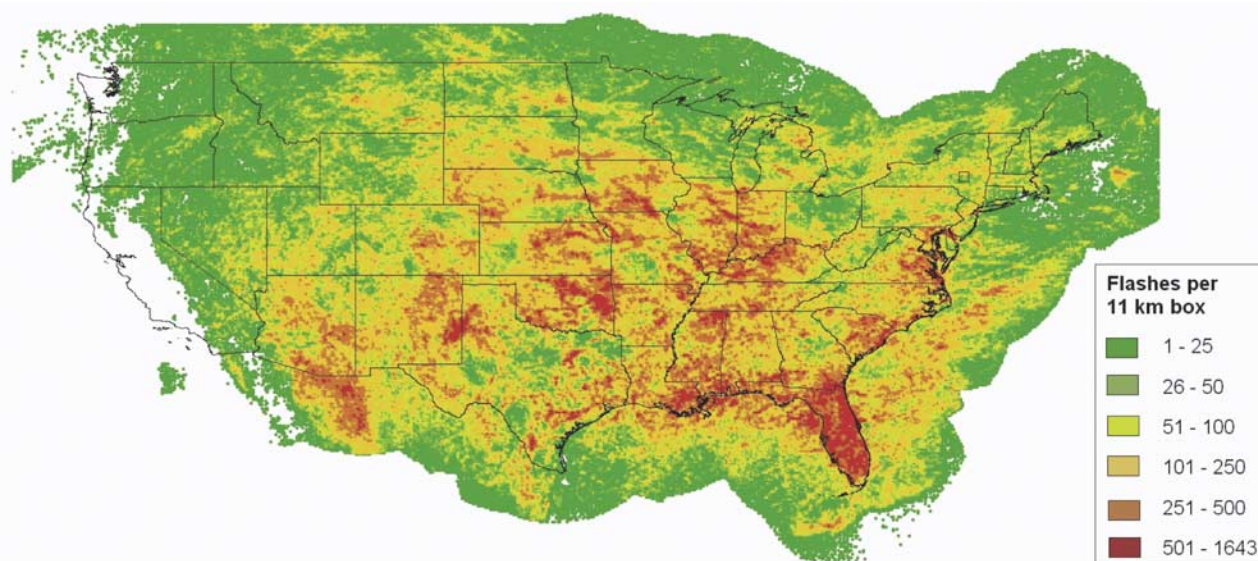


Figure 16. Flash densities of cloud-to-ground lightning during the complete INTEX-NA period between 1 July and 15 August 2004. Flashes are counted within boxes that are 11 km on each side.

[45] Convection as defined by the GFS model could be erroneously placed, and it does not indicate the presence of lightning. Our visual comparison between GFS-derived convection and NLDN CG lightning revealed that the GFS sometimes indicated deep convection in areas with no CG lightning and vice versa. In many of these cases the GFS had merely misplaced the convection. Generally speaking, however, areas of intense lightning corresponded to areas of GFS convection. The relationship between GFS convection and NLDN lightning certainly deserves a much more thorough investigation.

[46] In light of the previous comments, we computed encounters with NLDN-derived CG lightning in addition to encounters with GFS-derived convection. Our procedure has similarities to that used by *Jeker et al.* [2000]. A trajectory was considered to be lightning “influenced” if there was at least one NLDN-detected CG flash within 0.5° (or 1.5°) latitude/longitude and within ± 30 min of its position. Another set of statistics was compiled for trajectories encountering 60 or more flashes within these same spatial and temporal limits. The distances of 0.5 and 1.5° account for uncertainties in trajectory locations which generally increase with time. The arbitrary choices of one and 60 flashes consider the in-cloud lightning not detected by the NLDN and the fact that the chemical signature from a small number of flashes can be detected if the aircraft is near those flashes, while at more distant locations, much more lightning would have to occur before detection is possible because of the effects of diffusion over time. Figure 19 shows histograms of hourly flash counts over the entire INTEX period for areas of 0.5 and 1.5° . Most of the cells have less than 15 flashes. The ratio of the sum of grid cells having > 60 flashes to the total number of cells increases from 1% at 0.5° to 4% at 1.5° . If only cells containing flashes are considered (not the total number), the ratio increases from 15% to 30%. Our combination of four

criteria should be considered a reasonable range of scenarios producing lightning encounters in the DC-8 samples.

[47] As an example of the lightning encounter procedure, Figure 20a shows the track of DC-8 flight 7 on 12 July, as well as lightning that is color coded by age on the basis of the time between the lightning encounter and sampling by the DC-8. The trajectories linking the flight track to the lightning are not shown to facilitate viewing. In this example, one flash within a 1° area was considered an encounter. Flight 7 sampled air with a recent lightning influence (e.g., within 24 hours of DC-8 sampling, colored red or orange) due to storms over the Dakotas, Missouri, eastern Tennessee, and eastern Georgia. More aged convective and lightning influences also were sampled from storms on previous days over the Midwest, Gulf Coast, and Gulf of Mexico. Similarly, flight 12 (Figure 20b) sampled recently lightning influenced air (< 24 hours) from storms over eastern Kentucky, Tennessee, southeastern Georgia, and the lower Mississippi River Valley. Much older lightning influenced air (3–4 days prior) was sampled from storms over the Midwest and northeastern states. These two flights clearly indicate that the DC-8 sampled lightning byproducts having a variety of ages over a variety of geographical locations (e.g., lofted over cities, forests, etc). INTEX-NA

Table 2. Cloud-to-Ground Lightning Flashes Within the Area $66\text{--}126^\circ\text{W}$, $25\text{--}50^\circ\text{N}$ During the 6 Week INTEX-A Period (1 July to 15 August)^a

Year	1–31 Jul	1–15 Aug	1 Jul to 15 Aug
2003	7,329,890	3,549,906	10,879,796
2004	7,691,566	3,001,042	10,692,608
2005	6,873,867	3,871,840	10,745,707

^aFlashes less than 15 kA are not included since they are believed to represent intracloud discharges (K. Cummins, Vaisala, Inc., personal communication, January 2006).

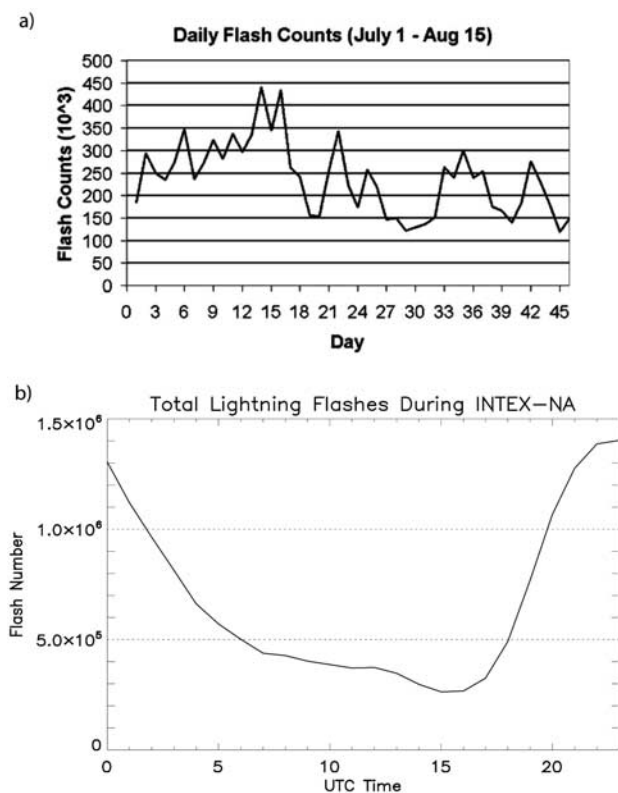


Figure 17. (a) Daily counts of cloud-to-ground lightning within the area 66–126°W, 25–50°N. Day 1 denotes 1 July 2004. (b) Diurnal distribution of cloud-to-ground lightning (UTC) within the area 66–126°W, 25–50°N.

papers providing detailed discussions of precipitation, convective, and lightning chemical signatures include *Bertram et al.* [2007], *Garrett et al.* [2006], A. Fried et al. (The role of convection in redistributing formaldehyde to the upper troposphere over North America and the North Atlantic during the summer 2004 INTEX campaign, manuscript in preparation, 2007) and M. Bükler et al. (Convective initiation of long-range stratospheric influence during INTEX-NA: Local ozone flux values, unpublished manuscript, 2007).

[48] Parcels sampled by the DC-8 often were impacted by fires in Alaska and western Canada. To quantify these encounters, MODIS-derived fire count data at weekly intervals (e.g., 1–7 July, 8–14 July, etc.) were obtained from the MODIS Rapid Response System at the University of Maryland (<http://maps.geog.umd.edu/maps.asp>). Then, trajectory locations at hourly intervals were compared to locations of the fires for that particular week. An encounter was assumed if a trajectory was within 0.5° and ±30 min of its position of a fire. To account for trajectory uncertainty, a second set of encounters was calculated using a search radius of 1.5°. This range of proximities is similar to that used for the NLDN data. The altitudes of trajectories over the fires were not considered because of the wide range of injection heights described earlier.

[49] Results of the encounter procedure are quite interesting (Table 3). Almost half of the DC-8’s trajectories encountered the PBL and/or the residual layer during the 10 day runs. Many of these encounters occurred during low-

level flight legs (not shown). One should note that no large-scale model, including the GFS, represents the individual elements of turbulence; only the parameterized effects are included. Nonetheless, pollutants lofted from near the surface by processes resolvable by the GFS model were sampled frequently by the DC-8 during INTEX.

[50] The DC-8 seldom sampled “pure” stratospheric air (i.e., air above the tropopause) (Table 3). Only 27% of the trajectories exceeded the tropopause height during the entire 10 day period. However, our simple diagnostic approach does not adequately consider stratospheric air that had been mixed into the lower levels by turbulence associated with tropopause folding, the jet stream, or other mechanisms. In-flight discussions suggested numerous occasions when the samples appeared to contain a stratospheric influence. *Tarasick et al.* [2007] and A. M. Thompson et al. (personal communication, 2005), both in this special section, discuss stratospheric contributions to INTEX-NA observations. Finally, one should note that most of the DC-8 trajectories passed over land during the previous 10 days; that is, only 6% remained over water during the entire period. Approximately 70% of the parcels either were sampled over land or encountered land within 6 hours of sampling. Thus the INTEX-NA chemical data are heavily influenced by land-based processes where the radiation profiles are different and there are distinct emissions and chemical processes.

[51] Only 8% of the DC-8’s trajectories did not encounter GFS-derived convection during the 10 day run period. Many of these convective encounters occurred during the first day, e.g., 21% during the first 6 hours and 46% during the first 24 hours. The percentages are less than 7% at each later period. These results indicate that many of the DC-8 samples exhibit a recent convective influence.

[52] Table 3 also presents results from the four criteria used to estimate lightning encounters for the combination of all eighteen DC-8 science flights. No data are presented beyond 120 hours since many trajectories by this time were in regions with insufficient NLDN data. The results vary considerably depending on how close the DC-8’s trajectory must be to the flash to be considered an encounter (within 0.5 or 1.5°), and on the number of flashes that must be contained within that search region (1 or 60 flashes). At 6 hours back, the NLDN-derived encounter values range from 2% to 18% compared to 21% from the GFS. At 24 and 48 hours back the two procedures give approximately the same percentages of encounters (mostly ~6%). At even earlier times, i.e., beyond 60 hours, encounters based on NLDN data are less than those from the GFS, possibly because some trajectories already extended beyond the domain of the NLDN data. At the end of the 120 hour period, from 28% to 65% of the trajectories had experienced NLDN lightning, while 81% had encountered GFS-defined convection. These statistics confirm that the DC-8 often flew near active deep convection, and that lightning induced NO_x likely is an important constituent of the INTEX samples, as described by *Bertram et al.* [2007] during INTEX-NA.

[53] The last two columns in Table 3 quantify the number of DC-8 samples that had been near wildfires in Alaska or western Canada. The backward trajectories indicate that no samples had been near Alaskan/Canadian fires during the most recent 24 hours because the DC-8 flight tracks never

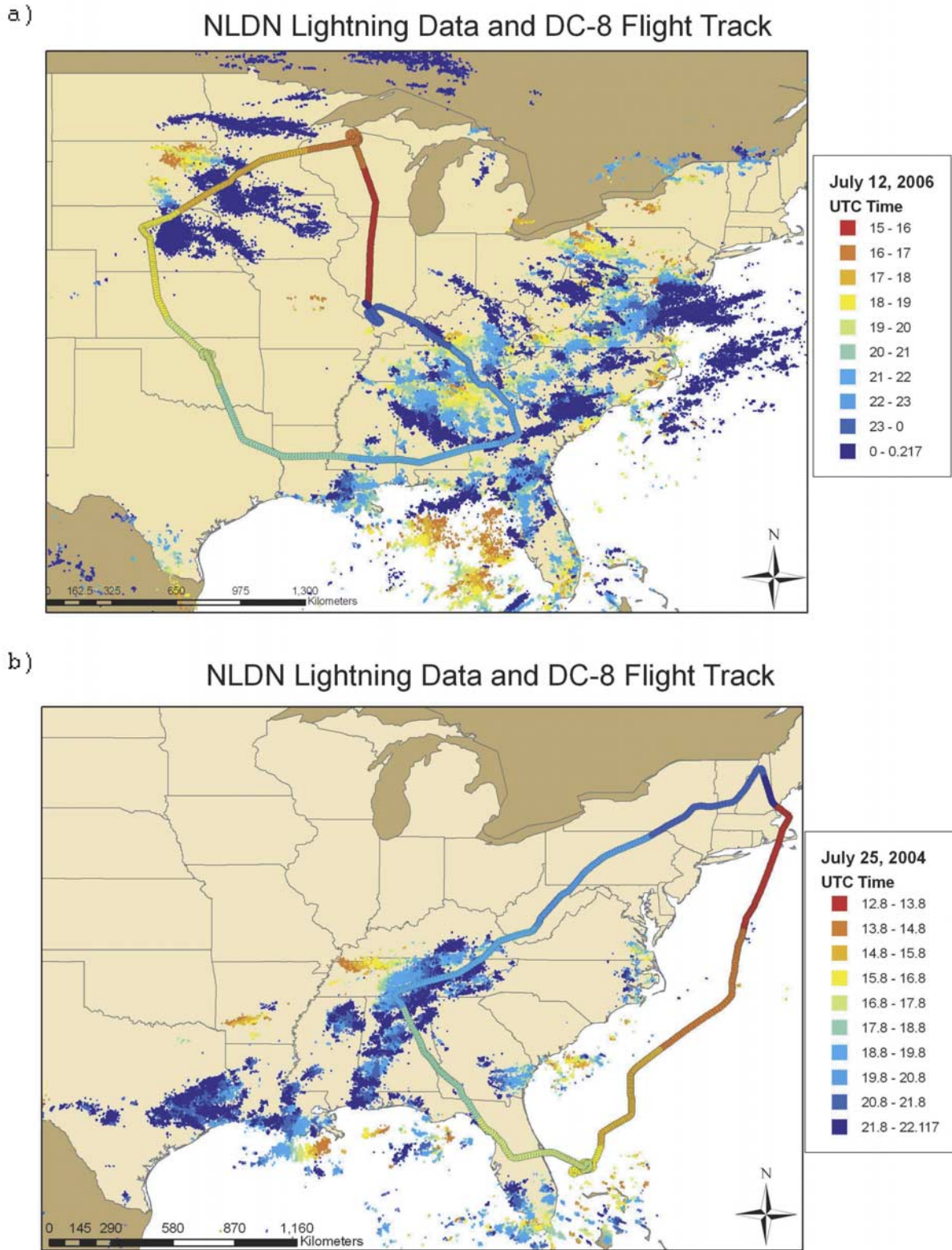


Figure 18. (a) Flight track of the DC-8 on 12 July 2004 (flight 7), where the different colors represent locations of the aircraft over 1 hour time segments. CG lightning in 1 hour time segments is shown in the same color scheme. (b) As in Figure 18a but for 25 July 2004 (flight 12).

Table 3. Percentage of Back Trajectories for All INTEX Flights Combined That Encountered Either the Planetary Boundary Layer (PBL), the Residual Layer, the Stratosphere (Strat), Convection Based on GFS Analysis Data, Lightning Based on Either 1 or 60 NLDN-Derived Flashes Within 0.5 or 1.5° Latitude, and Wildfires in Alaska or Western Canada Within 0.5 or 1.5° Latitude Before in Situ Sampling by the DC-8^a

Time Back, hours	PBL	Residual Layer	Strat	Over Land	Convection From GFS	Lightning, 1 NLDN, 0.5°	Lightning, 1 NLDN, 1.5°	Lightning, 60 NLDN, 0.5°	Lightning, 60 NLDN, 1.5°	Intercepted Fires, 0.5°	Intercepted Fires, 1.5°
6.0	20.5	11.4	5.5	69.4	21.4	8.2	17.7	2.4	7.9	0.0	0.0
12.0	0.5	7.3	2.0	5.1	9.1	4.8	8.2	1.6	4.0	0.0	0.0
18.0	2.3	2.4	1.6	4.2	9.3	6.4	9.5	2.6	6.6	0.4	0.0
24.0	2.2	1.3	1.9	3.2	6.6	6.1	6.7	3.3	6.1	0.2	0.4
36.0	1.3	3.7	2.4	3.4	9.9	5.4	5.5	3.1	4.6	0.4	1.6
48.0	4.0	2.4	1.7	2.1	7.0	7.8	9.1	4.2	8.1	1.2	2.7
60.0	1.1	2.9	2.1	1.4	4.4	4.0	2.5	2.9	3.8	1.7	1.9
72.0	2.9	2.0	1.3	0.9	3.7	4.0	2.7	3.0	4.0	2.1	2.9
96.0	2.9	4.0	1.8	1.1	6.3	2.7	2.2	2.9	2.3	2.3	3.3
120.0	2.4	2.6	1.6	0.9	3.5	1.7	1.1	1.9	1.7	1.3	2.1
Influence < 120 hours	40.1	40.0	21.9	91.7	81.2	51.1	65.2	27.9	49.1	9.6	14.9
144.0	1.9	2.0	1.0	0.8	2.9					1.5	2.4
168.0	1.7	2.2	1.5	0.3	2.5					1.5	1.9
192.0	2.1	2.2	1.1	0.3	2.1					1.6	1.9
216.0	1.6	1.7	1.0	0.4	2.1					1.3	1.3
240.0	1.0	1.0	0.9	0.1	1.0					0.4	0.7
Influence < 240 hours	48.4	49.1	27.4	93.6	91.8	51.1	65.2	27.9	49.1	15.8	23.0
No Influence	51.6	50.9	72.6	6.4	8.2	48.9	34.8	72.1	50.9	84.2	77.0

^aFor the four NLDN columns, the encounters only extend through 120 hours. Once a back trajectory encountered one of these conditions, subsequent encounters within the same category were not counted.

were that close to the fire locations. Instead, the encounters are greatest for fires located ~48 to 144 hours upwind of the sampled locations. Approximately 10% to 15% of the DC-8 samples had been over fire locations during the previous 120 hours (5 days), depending on the search radius being considered. By the end of the 10 day period, ~80% of the samples had not passed over fire locations, whereas ~20% of the samples had passed near fires over Alaska or Canada. Thus again it is clear that the record number of fires in these areas often were sampled by the DC-8 at distant locations.

6. Conclusions

[54] This paper has described meteorological conditions during the Intercontinental Chemical Transport Experiment–North America (INTEX-NA) which was conducted over the contiguous United States and adjacent areas during July and August 2004. Anomalously strong and persistent high pressure dominated Alaska and western Canada during much of the INTEX-NA period. This blocking pattern prevented low-pressure areas over the North Pacific from bringing cooler temperatures and abundant precipitation to Alaska. The result was unusually hot and dry conditions over much of the area. Relatively zonal flow dominated the contiguous United States during the first 2 weeks of the mission, while a series of large amplitude troughs traversed the eastern half of the country during the final 4 weeks. Several of these troughs extended the full north to south length of the eastern United States, reaching over the Gulf of Mexico.

[55] The unusually strong middle tropospheric troughs were accompanied by a series of cold fronts that also reached as far south as the Gulf of Mexico. Fronts extending

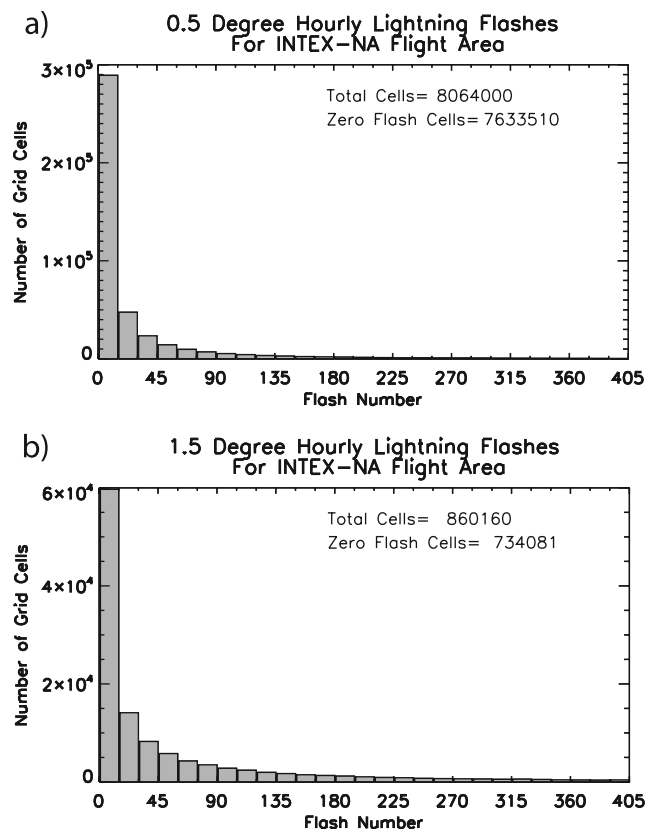
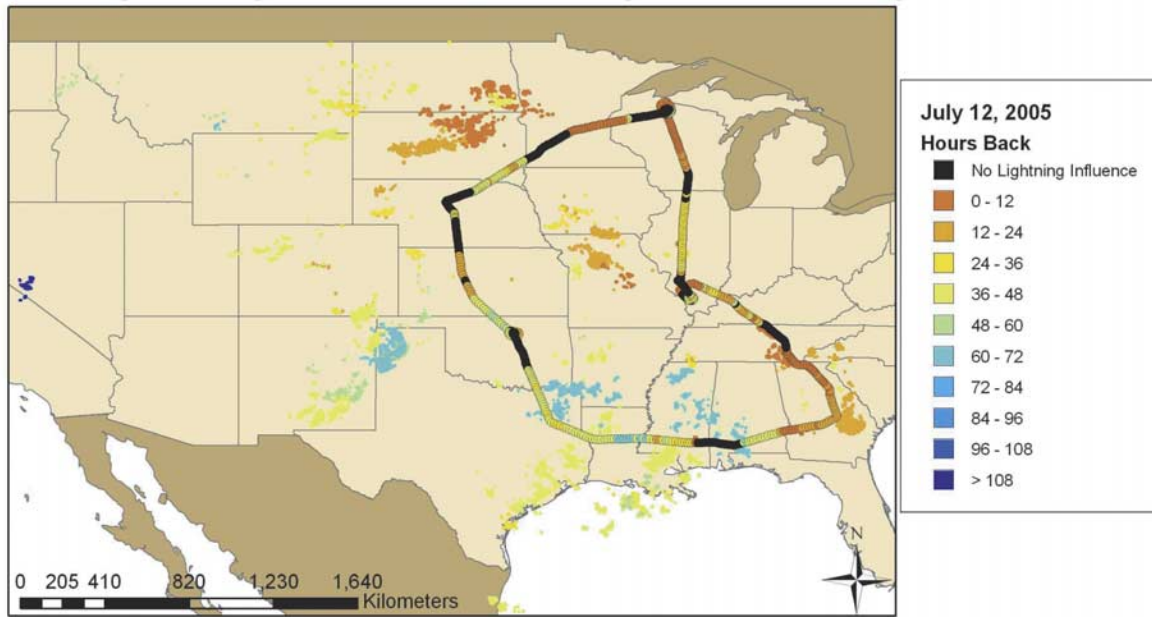


Figure 19. Histograms of hourly lightning flashes within (a) 0.5° latitude boxes and (b) 1.5° latitude boxes for all hours between 1 July and 15 August over the INTEX domain (66–126°W, 25–50°N).

a) **Lightning Influence on Flight Level Trajectories**



b)

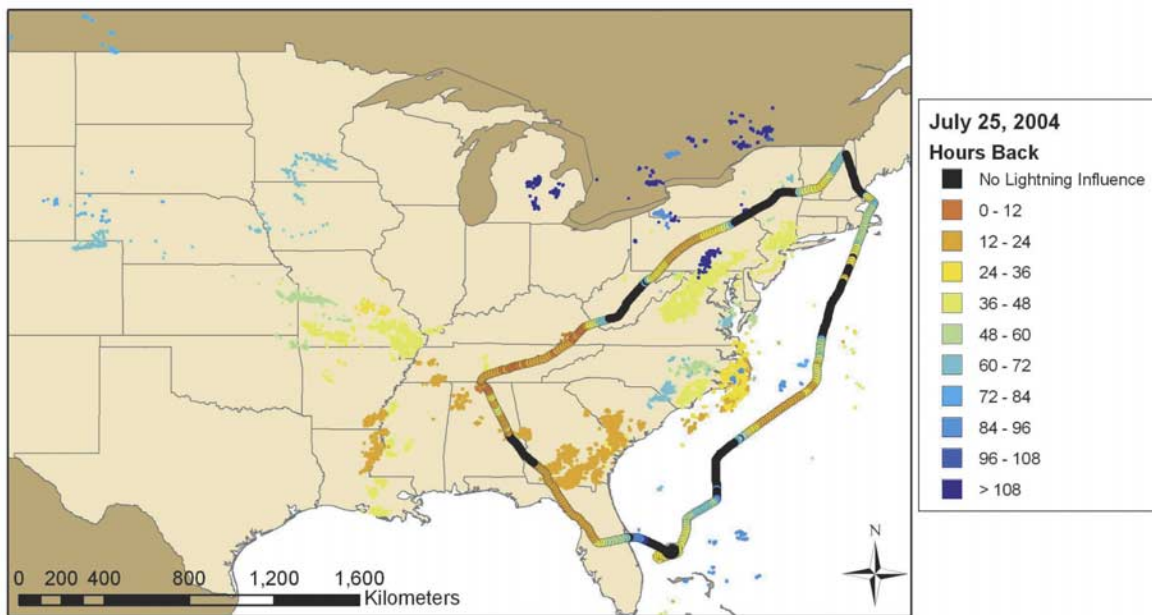


Figure 20. Locations where backward trajectories from the DC-8 at 1 min intervals intercepted cloud-to-ground lightning flashes during 9–12 July 2004. At least one NLDN flash had to occur within a 1° radius and 1 hour window of the trajectory to be included. The various colors represent the hours back from the flight track before the lightning encounter. The DC-8 flight track and its altitude on 12 July are superimposed.

this far south during the summer are uncommon. During the INTEX-NA period, seven cold fronts passed Atlanta, Georgia, the greatest number during the 2000–2005 period. These fronts brought record low temperatures to portions of the Great Plains and south. Frontal passages over the northeast were only somewhat above average, but the short average time interval between passages (4.6 days) meant

that stagnant high-pressure centers containing abundant pollution never formed over the area.

[56] The persistent high pressure over Alaska provided ideal conditions for wildfires in Alaska and western Canada. As a result, a record number of acres was burned during summer 2004, surpassing the old record established in 1957. The location of the persistent ridge also meant that

burning by-products often were transported southeastward toward the contiguous United States and the INTEX domain. These plumes were sampled by the DC-8 during numerous flights. Back trajectories revealed that ~20% of the DC-8 samples had been near fires in Alaska or western Canada during the previous 10 days. During some flights, forward trajectories and satellite imagery showed that the plumes later were carried to parts of Europe, Africa, and even the Arctic. In some cases the transported pollution near Europe was sampled in a quasi-Lagrangian sense by INTEX's international partners participating in the ICARTT experiment. It is clear that the atmospheric chemistry during INTEX-NA was heavily influenced by the record-breaking fires and the long-range transport of their by-products.

[57] Cloud to ground (CG) lightning data showed that horizontal patterns and numbers of lightning flashes during INTEX-NA were similar to those of 2003 and 2005. Statistics derived from backward trajectories indicated that between 28% and 65% of the DC-8 samples had been near CG lightning during the previous 5 days. If convection derived from the GFS meteorological model is considered, the DC-8 sampled convectively influenced air ~81% of the time within 5 days of DC-8 sampling, with many of these encounters occurring within 6 hours of in situ sampling. It is clear that deep convection and lightning were important factors during INTEX-NA.

[58] In conclusion, INTEX-NA was a period of active weather. The period exhibited several meteorologically anomalous aspects that should be considered when comparing its chemical measurements with those from other periods. Furthermore, these anomalies suggest the need for future missions that would sample more typical conditions, e.g., stagnant conditions over the northeast and the long-range transport of the accumulated pollutants.

[59] **Acknowledgments.** This research was sponsored by NASA's Tropospheric Chemistry Program under grants NNG04GC33G and NNG06B43G to Florida State University. The NLDN lightning data were provided courtesy of the NASA Marshall Global Hydrology Resource Center using data obtained from Vaisala Inc. We appreciate the helpfulness of the DC-8 crews and support staff during the INTEX-A preparation and deployment periods that allowed us to satisfy our science objectives. Finally, the anonymous reviewers had many ideas for clarifying the original manuscript.

References

- Andreae, M. O., D. Rosenfeld, P. Artaxo, A. A. Costa, G. P. Frank, K. M. Longo, and M. A. F. Dias (2004), Smoking rain clouds over the Amazon, *Science*, *303*, 1337–1342.
- Arakawa, A., and W. H. Schubert (1974), Interaction of a cumulus ensemble with the large-scale environment, Part I, *J. Atmos. Sci.*, *31*, 674–704.
- Bertram, T. H., et al. (2007), Direct measurements of the convective recycling of the upper troposphere, *Science*, *315*(5813), 816–820.
- Blake, N. J., et al. (2001), Large scale latitudinal distribution of NMHCs and selected halocarbons in the troposphere over the Pacific Ocean during the March–April 1999 Pacific Exploratory Expedition (PEM-Tropics B), *J. Geophys. Res.*, *106*, 32,627–32,644.
- Boccippio, D. J., K. L. Cummins, H. J. Christian, and S. J. Goodman (2001), Combined satellite- and surface-based estimation of the intra-cloud cloud-to-ground lightning ratio over the continental United States, *Mon. Weather Rev.*, *129*, 108–122.
- Bond, D. W., R. Zhang, X. Tie, G. Brasseur, G. Huffines, R. E. Orville, and D. J. Boccippio (2001), NO_x production by lightning over the continental United States, *J. Geophys. Res.*, *106*, 27,701–27,710.
- Carlson, T. N. (1998), *Mid-Latitude Weather Systems*, Am. Meteorol. Soc., Boston, Mass.
- Cohan, D. S., M. G. Schultz, and D. J. Jacob (1999), Convective injection and photochemical decay of peroxides in the tropical upper troposphere: Methyl iodide as a tracer of marine convection, *J. Geophys. Res.*, *104*, 5717–5724.
- Colarco, P. R., M. R. Schoeberl, B. G. Doddridge, L. T. Marufu, O. Torres, and E. J. Welton (2004), Transport of smoke from Canadian forest fires to the surface near Washington, D.C.: Injection height, entrainment, and optical properties, *J. Geophys. Res.*, *109*, D06203, doi:10.1029/2003JD004248.
- Cooper, O. R., et al. (2004), A case study of transpacific warm conveyor belt transport: Influence of merging airstreams on trace gas import to North America, *J. Geophys. Res.*, *109*, D23S08, doi:10.1029/2003JD003624.
- Cooper, O. R., et al. (2006), Large upper tropospheric ozone enhancements above midlatitude North America during summer: In situ evidence from the IONS and MOZAIC ozone measurement network, *J. Geophys. Res.*, *111*, D24S05, doi:10.1029/2006JD007306.
- Cummins, K. L., M. J. Murphy, E. A. Bardo, W. L. Hiscox, R. B. Pyle, and A. E. Pifer (1998), A combined TOA/MDF technology upgrade of the U.S. National Lightning Detection Network, *J. Geophys. Res.*, *103*, 9035–9044.
- Cummins, K. L., J. A. Cramer, C. J. Biagi, E. P. Krider, J. Jerauld, M. A. Uman, and V. A. Rakov (2006), The U.S. national lightning detection network: Post-upgrade status, paper presented at 2nd Conference on Meteorological Applications of Lightning Data, Am. Meteorol. Soc., Atlanta, Ga.
- Damoah, R., N. Spichtinger, C. Forster, P. James, I. Mattis, U. Wandinger, S. Beirle, T. Wagner, and A. Stohl (2004), Around the world in 17 days—Hemispheric-scale transport of forest fire smoke from Russia in May 2003, *Atmos. Chem. Phys.*, *4*, 1311–1321.
- Damoah, R., N. Spichtinger, R. Servranckx, M. Fromm, E. W. Eloranta, I. A. Rازenkov, P. James, M. Shulsi, C. Forster, and A. Stohl (2005), Transport modeling of a pyro-convection event in Alaska, *Atmos. Chem. Phys. Disc.*, *5*, 6185–6214.
- Damoah, R., N. Spichtinger, R. Servranckx, M. Fromm, E. W. Eloranta, I. A. Rازenkov, P. James, M. Shulsi, C. Forster, and A. Stohl (2006), A case study of pyro-convection using transport model and remote sensing data, *Atmos. Chem. Phys.*, *6*, 173–185.
- DeBell, L. J., R. W. Talbot, J. E. Dibb, J. W. Munger, E. V. Fischer, and S. E. Frolking (2004), A major regional air pollution event in the northeastern United States caused by extensive forest fires in Quebec, Canada, *J. Geophys. Res.*, *109*, D19305, doi:10.1029/2004JD004840.
- DeCaria, A. J., K. E. Pickering, G. L. Stenchikov, J. R. Scala, J. L. Stith, J. E. Dye, B. A. Ridley, and P. Laroche (2000), A cloud-scale model study of lightning-generated NO_x in an individual thunderstorm during STERAO-A, *J. Geophys. Res.*, *105*, 11,601–11,616.
- DeCaria, A. J., K. E. Pickering, G. L. Stenchikov, and L. E. Ott (2005), Lightning-generated NO_x and its impact on tropospheric ozone production: A three-dimensional modeling study of a Stratosphere-Troposphere Experiment: Radiation, Aerosols and Ozone (STERAO-A) thunderstorm, *J. Geophys. Res.*, *110*, D14303, doi:10.1029/2004JD005556.
- Deeter, M. N., et al. (2003), Operational carbon monoxide retrieval algorithm and selected results for the MOPITT instrument, *J. Geophys. Res.*, *108*(D14), 4399, doi:10.1029/2002JD003186.
- de Gouw, J. A., et al. (2006), Volatile organic compounds composition of merged and aged forest fire plumes from Alaska and western Canada, *J. Geophys. Res.*, *111*, D10303, doi:10.1029/2005JD006175.
- Eckhardt, S., A. Stohl, H. Wernli, P. James, C. Forster, and N. Spichtinger (2004), A 15-year climatology of warm conveyor belts, *J. Clim.*, *17*, 218–237.
- Fehr, T., H. Höller, and H. Huntrieser (2004), Model study on production and transport of lightning-produced NO_x in a EULINOX supercell storm, *J. Geophys. Res.*, *109*, D09102, doi:10.1029/2003JD003935.
- Fehsenfeld, F. C., et al. (2006), International Consortium for Atmospheric Research on Transport and Transformation (ICARTT): North America to Europe—Overview of the 2004 summer field study, *J. Geophys. Res.*, *111*, D23S01, doi:10.1029/2006JD007829.
- Forster, C., et al. (2001), Transport of boreal forest fire emissions from Canada to Europe, *J. Geophys. Res.*, *106*, 22,817–22,906.
- Fromm, M. D., and R. Servranckx (2003), Transport of forest fire smoke above the tropopause by supercell convection, *Geophys. Res. Lett.*, *30*(10), 1542, doi:10.1029/2002GL016820.
- Fromm, M., J. Alfred, K. Hoppel, J. Hornstein, R. Bevilacqua, E. Shettle, R. Servranckx, Z. Li, and B. Stocks (2000), Observations of boreal forest fire smoke in the stratosphere by POAM III, SAGE II, and lidar in 1998, *Geophys. Res. Lett.*, *27*, 1407–1410.
- Fromm, M., R. Bevilacqua, R. Servranckx, J. Rosen, J. P. Thayer, J. Herman, and D. Larko (2005), Pyro-cumulonimbus injection of smoke to the stratosphere: Observations and impact of a super blowup in northwestern Canada on 3–4 August 1998, *J. Geophys. Res.*, *110*, D08205, doi:10.1029/2004JD005350.
- Fuelberg, H. E., R. O. Loring Jr., M. V. Watson, M. C. Sinha, K. E. Pickering, A. M. Thompson, G. W. Sachse, D. R. Blake, and M. R. Schoeberl (1996), TRACE-A trajectory intercomparison: 2. Isentropic and kinematic methods, *J. Geophys. Res.*, *101*, 23,927–23,939.

- Fuelberg, H. E., R. E. Newell, S. P. Longmore, W. Zhu, D. J. Westberg, E. V. Browell, D. R. Blake, G. L. Gregory, and G. W. Sachse (1999), A meteorological overview of the PEM-Tropics period, *J. Geophys. Res.*, *104*, 5585–5622.
- Fuelberg, H. E., J. R. Hannan, P. F. J. van Velthoven, E. V. Browell, G. Bieberbach Jr., R. D. Knabb, G. L. Gregory, K. E. Pickering, and H. B. Selkirk (2000), A meteorological overview of the SONEX period, *J. Geophys. Res.*, *105*, 3633–3651.
- Fuelberg, H. E., C. M. Kiley, J. R. Hannan, D. J. Westberg, M. A. Avery, and R. E. Newell (2003), Atmospheric transport during the Transport and Chemical Evolution over the Pacific TRACE-P experiment, *J. Geophys. Res.*, *108*(D20), 8782, doi:10.1029/2002JD003092.
- Garrett, T. J., L. Avey, P. I. Palmer, A. Stohl, J. A. Neuman, C. A. Brock, T. B. Ryerson, and J. S. Holloway (2006), Quantifying wet scavenging processes in aircraft observations of nitric acid and cloud condensation nuclei, *J. Geophys. Res.*, *111*, D23S51, doi:10.1029/2006JD007416.
- Grell, G. A. (1993), Prognostic evaluation of assumptions used by cumulus parameterizations, *Mon. Weather Rev.*, *121*, 764–787.
- Hong, S.-Y., and H.-L. Pan (1996), Nonlocal boundary layer vertical diffusion in a medium-range forecast model, *Mon. Weather Rev.*, *124*, 2322–2339.
- Immler, F., D. Engelbart, and O. Schrems (2005), Fluorescence from atmospheric aerosol detected by a lidar indicates biogenic particles in the stratosphere, *Atmos. Chem. Phys.*, *5*, 345–355.
- Jaffe, D., I. Bertsch, L. Jaeglé, P. Novelli, J. S. Reid, H. Tanimoto, R. Vingarzan, and D. L. Westphal (2004), Long-range transport of Siberian biomass burning emissions and impact on surface ozone in western North America, *Geophys. Res. Lett.*, *31*, L16106, doi:10.1029/2004GL020093.
- Jeker, D. P., L. Pfister, A. M. Thompson, D. Brunner, D. J. Boccippio, K. E. Pickering, H. Wernli, Y. Kondo, and J. Staehelin (2000), Measurements of nitrogen oxides at the tropopause: Attribution to convection and correlation with lightning, *J. Geophys. Res.*, *105*(D3), 3679–3700.
- Jost, H. J., et al. (2004), In situ observations of mid-latitude forest fire plumes deep in the stratosphere, *Geophys. Res. Lett.*, *31*, L11101, doi:10.1029/2003GL019253.
- Kalnay, E., et al. (1996), The NCEP/NCAR reanalysis 40-year project, *Bull. Am. Meteorol. Soc.*, *77*, 437–471.
- Kato, S., P. Pochanart, J. Hirokawa, Y. Kajii, H. Akimoto, Y. Ozaki, K. Obi, T. Katsuno, D. G. Streets, and N. P. Minko (2002), The influence of Siberian forest fires on carbon monoxide concentrations at Happo, Japan, *Atmos. Environ.*, *36*, 385–390.
- Kiley, C. M., and H. E. Fuelberg (2006), An examination of summertime cyclone transport processes during Intercontinental Chemical Transport Experiment (INTEX-A), *J. Geophys. Res.*, *111*, D24S06, doi:10.1029/2006JD007115.
- Lawrence, M. G., et al. (1994), Lightning and atmospheric chemistry: The rate of NO_x production in 1994, in *Handbook of Atmospheric Electrodynamics*, edited by H. Volland, pp. 189–202, Radioastron. Inst., Univ. of Bonn, Bonn, Germany.
- Lericos, T. P., H. E. Fuelberg, A. I. Watson, and R. L. Holle (2002), Warm season lightning distributions over the Florida peninsula as related to synoptic patterns, *Weather Forecasting*, *17*, 83–98.
- Livesey, N. J., M. D. Fromm, J. W. Waters, G. L. Manney, M. L. Santee, and W. G. Read (2004), Enhancements in lower stratospheric CH₃CN observed by the Upper Atmosphere Research Satellite Microwave Limb Sounder following boreal forest fires, *J. Geophys. Res.*, *109*, D06308, doi:10.1029/2003JD004055.
- Maloney, J. C., H. E. Fuelberg, M. A. Avery, J. H. Crawford, D. R. Blake, B. G. Heikes, G. W. Sachse, S. T. Sandholm, H. Singh, and R. W. Talbot (2001), Chemical characteristics of air from different source regions during the second Pacific Exploratory Mission in the Tropics (PEM-Tropics B), *J. Geophys. Res.*, *106*, 32,609–32,625.
- Martin, B. D., H. E. Fuelberg, N. J. Blake, J. H. Crawford, J. A. Logan, D. R. Blake, and G. W. Sachse (2002), Long range transport of Asian outflow to the equatorial Pacific, *J. Geophys. Res.*, *108*(D2), 8322, doi:10.1029/2001JD001418.
- Mauzerall, D. L., J. A. Logan, D. J. Jacob, B. E. Anderson, D. R. Blake, J. D. Bradshaw, B. Heikes, G. W. Sachse, H. Singh, and R. Talbot (1998), Photochemistry in biomass burning plumes and implications for tropospheric ozone over the tropical South Atlantic, *J. Geophys. Res.*, *103*, 8401–8423.
- McKeen, S. A., G. Wotawa, D. D. Parrish, J. S. Holloway, M. P. Buhr, G. Hübler, F. C. Fehsenfeld, and J. F. Meagher (2002), Ozone production from Canadian wildfires during June and July of 1995, *J. Geophys. Res.*, *107*(D14), 4192, doi:10.1029/2001JD000697.
- McNeal, R. J., J. P. Mugler Jr., R. C. Harriss, and J. M. Hoell Jr. (1984), NASA Global Tropospheric Experiment, *Eos Trans. AGU*, *64*, 561–562.
- Merrill, J. T., R. E. Newell, and A. S. Bachmeier (1997), A meteorological overview for the Pacific Exploratory Mission—West Phase B, *J. Geophys. Res.*, *102*, 28,241–28,253.
- Morris, G. A., et al. (2006), Alaskan and Canadian forest fires exacerbate ozone pollution over Houston, Texas, on 19 and 20 July 2004, *J. Geophys. Res.*, *111*, D24S03, doi:10.1029/2006JD007090.
- Novelli, P. C., K. A. Masarie, P. M. Lang, B. D. Hall, R. C. Myers, and J. W. Elkins (2003), Reanalysis of tropospheric CO trends: Effects of the 1997–1998 wildfires, *J. Geophys. Res.*, *108*(D15), 4464, doi:10.1029/2002JD003031.
- Orville, R. E., and G. R. Huffines (2001), Cloud-to-ground lightning in the United States: NLDN results in the first decade, 1989–1998, *Mon. Weather Rev.*, *129*, 1179–1193.
- O’Sullivan, D., B. G. Heikes, M. Lee, W. Chang, G. L. Gregory, D. R. Blake, and G. W. Sachse (1999), Distribution of hydrogen peroxide and methylhydroperoxide over the Pacific and South Atlantic, *J. Geophys. Res.*, *104*, 5635–5646.
- Pan, H.-L., and W.-S. Wu (1995), Implementing a mass flux convection parameterization package for the NMC medium-range forecast model, *NMC Off. Note*, *409*, 40 pp., Natl. Cent. for Environ. Predict., Washington, D. C.
- Pfister, G., P. G. Hess, L. K. Emmons, J.-F. Lamarque, C. Wiedinmyer, D. P. Edwards, G. Petron, J. C. Gille, and G. W. Sachse (2005), Quantifying CO emissions from the 2004 Alaskan wildfires using MOPITT CO data, *Geophys. Res. Lett.*, *32*, L11809, doi:10.1029/2005GL022995.
- Pfister, G. G., et al. (2006), Ozone production from the 2004 North American boreal fires, *J. Geophys. Res.*, *111*, D24S07, doi:10.1029/2006JD007695.
- Price, C., J. Penner, and M. Prather (1997), NO_x from lightning: 2. Constraints from the global atmospheric electric circuit, *J. Geophys. Res.*, *102*, 5943–5952.
- Richmond, M. A., and T. L. Shy (2005), An extraordinary summer in the interior of Alaska, paper presented at 8th Conference on Polar Meteorology and Oceanography, Am. Meteorol. Soc., San Diego, Calif.
- Rozell, N. (2004), Smoked pike on menu for Yukon Flats scientists, *Alaska Sci. Forum*, 1710.
- Russell, P. B., et al. (2007), Multi-grid-cell validation of satellite aerosol property retrievals in INTEX/ITCT/ICARTT 2004, *J. Geophys. Res.*, doi:10.1029/2006JD007606, in press.
- Singh, H. B., W. H. Brune, J. H. Crawford, D. J. Jacob, and P. B. Russell (2006), Overview of the summer 2004 Intercontinental Chemical Transport Experiment—North America (INTEX-A), *J. Geophys. Res.*, *111*, D24S01, doi:10.1029/2006JD007905.
- Smith, J. R., H. E. Fuelberg, and A. I. Watson (2005), Warm season lightning distributions over the northern Gulf of Mexico coast and their relation to synoptic scale and mesoscale environments, *Weather Forecasting*, *20*, 415–438.
- Spichtinger, N., R. Damoah, S. Eckard, C. Forster, P. James, T. Beirle, T. Wagner, P. C. Novelli, and A. Stohl (2004), Boreal forest fires in 1997 and 1998: A seasonal comparison using transport model simulations and measurement data, *Atmos. Chem. Phys.*, *4*, 1857–1868.
- Stohl, A. (1998), Computation, accuracy, and applications of trajectories—A review and bibliography, *Atmos. Environ.*, *32*, 947–966.
- Stohl, A. (2001), A one-year Lagrangian “climatology” of airstreams in the northern hemisphere troposphere and lowermost stratosphere, *J. Geophys. Res.*, *106*(D7), 7263–7280.
- Stohl, A. (2006), Characteristics of atmospheric transport into the Arctic troposphere, *J. Geophys. Res.*, *111*, D11306, doi:10.1029/2005JD006888.
- Stohl, A., G. Wotawa, P. Seibert, and H. Kromp-Kolb (1995), Interpolation errors in wind fields as a function of spatial and temporal resolution and their impact on different types of kinematic trajectories, *J. Appl. Meteorol.*, *34*, 2149–2165.
- Tanimoto, H., Y. Kajii, J. Hirokawa, H. Akimoto, and N. P. Minko (2000), The atmospheric impact of boreal forest fires in far eastern Siberia on the seasonal variation of carbon monoxide: Observations at Richiri, a northern remote island in Japan, *Geophys. Res. Lett.*, *27*, 4073–4076.
- Tarasick, D. W., et al. (2007), Comparison of Canadian air quality forecast models with tropospheric ozone profile measurements above mid-latitude North America during the IONS/ICARTT campaign: Evidence for stratospheric input, *J. Geophys. Res.*, doi:10.1029/2006JD007782, in press.
- Tiedtke, M. (1983), The sensitivity of the time-mean large-scale flow to cumulus convection in the ECMWF model, paper presented at ECMWF Workshop on Convection in Large-Scale Models, Reading, U.K., 28 Nov. to 1 Dec.
- Troen, I., and L. Mahrt (1986), A simple model of the atmospheric boundary layer: Sensitivity to surface evaporation, *Boundary Layer Meteorol.*, *37*, 129–148.
- Turquetty, S., et al. (2007), Inventory of boreal fire emissions for North America in 2004: Importance of peat burning and pyroconvective injection, *J. Geophys. Res.*, *112*, D12503, doi:10.1029/2006JD007281.

- Wernli, H. (1997), A Lagrangian-based analysis of extratropical cyclones. II: A detailed case study, *Q. J. R. Meteorol. Soc.*, 123, 1677–1706.
- Wotawa, G., and M. Trainer (2000), The influence of Canadian forest fires on pollutant concentrations in the United States, *Science*, 288, 324–328.
- Wotawa, G., P. C. Novelli, M. Trainer, and C. Granier (2001), Inter-annual variability of summertime CO concentrations in the Northern Hemisphere explained by boreal forest forest in North America and Russia, *Geophys. Res. Lett.*, 28, 4575–4578.
- Yurganov, L. N., et al. (2004), A quantitative assessment of the 1998 carbon monoxide emission anomaly in the Northern Hemisphere based on total column and surface concentration measurements, *J. Geophys. Res.*, 109, D15305, doi:10.1029/2004JD004559.
-
- H. E. Fuelberg, J. J. Halland, C. M. Kiley, D. Morse, and M. J. Porter, Department of Meteorology, Florida State University, Tallahassee, FL 32306-4520, USA. (fuelberg@met.fsu.edu; jhalland@met.fsu.edu; ckiley@met.fsu.edu; dmorse@met.fsu.edu; mporter@met.fsu.edu)